AD-A059 932 IOWA INST OF HYDRAULIC RESEARCH IOWA CITY F/G 13/11
DETAILED MODEL STUDY OF PUMP-APPROACH FLOWS FOR THE LAKE CHICOT--ETC(U)
OCT 77 T NAKATO, J F KENNEDY
UNCLASSIFIED IIHR-208 NL

| OF |
AD
A059932

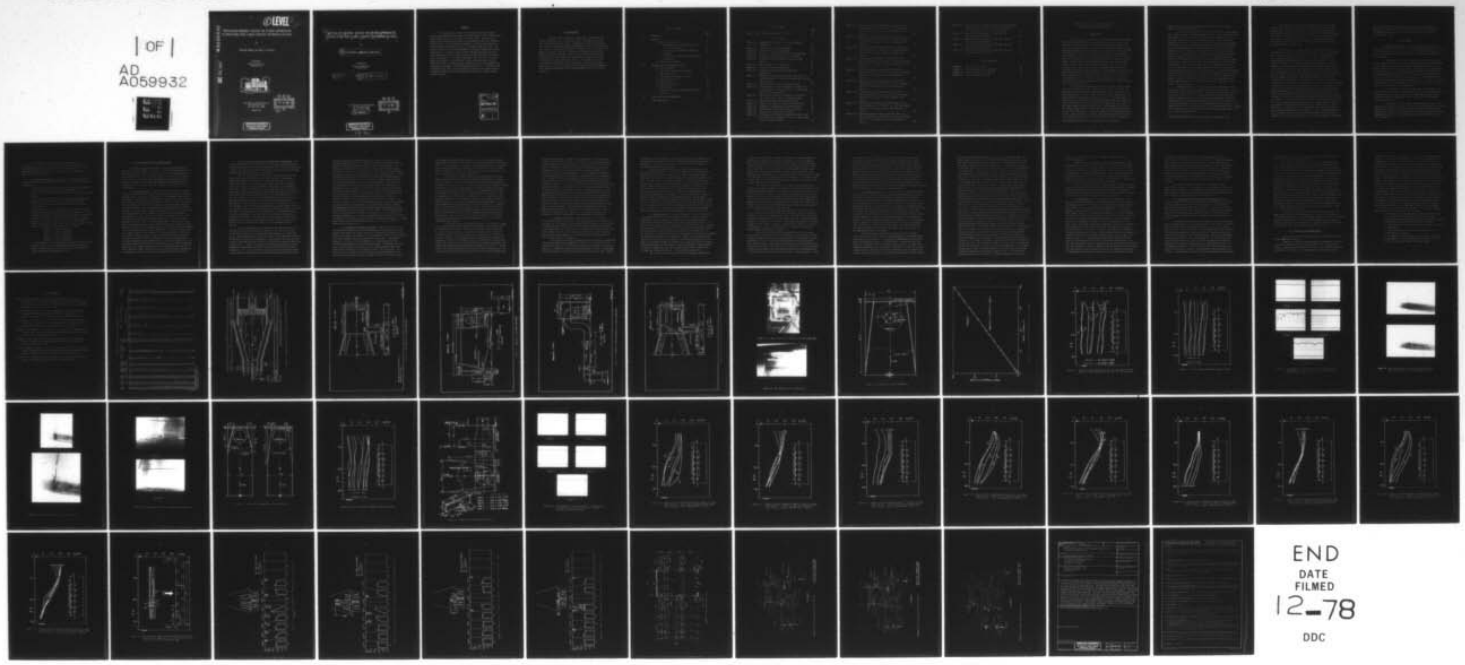

END
DATE
FILMED
12-78
DDC

(5) LEVEL II

DETAILED MODEL STUDY OF PUMP-APPROACH FLOWS FOR THE LAKE CHICOT PUMPING PLANT

by

Tatsuaki Nakato and John F. Kennedy

Submitted to

Stanley Consultants, Inc.
Muscatine, Iowa

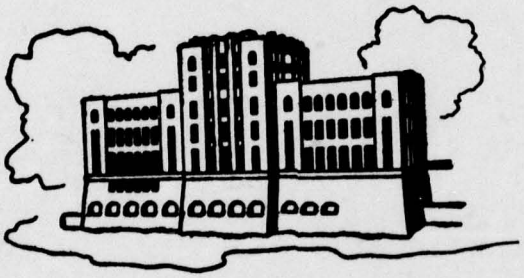

Iowa Institute of Hydraulic Research
The University of Iowa
Iowa City, Iowa 52242

October 1977

(6)

DETAILED MODEL STUDY OF PUMP-APPROACH FLOWS FOR THE LAKE CHICOT PUMPING PLANT,

by

(10) Tatsuaki Nakato and John F. Kennedy

Submitted to

Stanley Consultants, Inc.
Muscatine, Iowa

(12) 66 p.

(14) IIHR-208

Iowa Institute of Hydraulic Research
The University of Iowa
Iowa City, Iowa 52242

(11) October 1977

ABSTRACT

A 1:24 Froude-scale model of the proposed Lake Chicot Pumping Station was constructed and utilized to identify and to correct hydraulically objectionable features of the flows in the pump sumps. The model tests showed that the flows from the plant forebay generally enter the individual pump bays with a strong transverse component of velocity and produced an intense captive eddy on the lee side of each pump-bay partition wall. The transverse velocity resulted from geometric constraints imposed on the plant configuration. In order to achieve better pump approach-flow conditions trash racks with relatively deep vertical bars which functioned as turning vanes were proposed. A 1:10-scale sump model then was built to test for model-scale effects in the trash-rack tests, and an extensive study was conducted to obtain an improved sump configuration which would minimize any vortex-related problems in and around pump suction bells. The modified sump configuration has small clearance between the pump bell and sump back-wall; converging sidewalls; and a floor mounted splitter plate (vortex breaker) beneath the pump.

ACKNOWLEDGEMENTS

This model investigation was conducted for, and sponsored by, Stanley Consultants, Inc., of Muscatine, Iowa. The authors wish to express their special thanks to Mr. L. Lynn Pruitt of Stanley Consultants, Inc., for his unfailing cooperating throughout the course of the study and for critically reviewing the manuscript. Valuable input were received from members of the U.S. Army Corps of Engineers, Vicksburg District Office, Waterways Experimental Station, Office of Chief, and Lower Mississippi Valley Division. Their suggestions significantly influenced the course of the study and improved the final results. The authors also wish to acknowledge Mr. Dale Harris and his shop staff for modifying the model numerous times; Dr. John R. Glover for his assistance with the instrumentation; and Mr. Shih-Huang Chieh for conducting model tests as a research assistant.

TABLE OF CONTENTS

LIST OF TABLES

LIST OF FIGURES

LIST OF APPENDICES

DETAILED MODEL STUDY OF PUMP-APPROACH FLOWS FOR THE LAKE CHICOT PUMPING PLANT

I. INTRODUCTION

The hydraulic characteristics of the proposed Lake Chicot Pumping Plant have been investigated experimentally since May, 1975, at the Iowa Institute of Hydraulic Research. The report summarizing results of the tests on the general hydraulic performance of the proposed forebay and pump bays was submitted to Stanley Consultants, Inc., Muscatine, Iowa, in August, 1976 (Nakato and Kennedy 1976). Therein, potential prototype problems arising from the formation and persistence of intense suction-bell vortices, which were discovered in the 1:10-scale model sump, were discussed at some length. Concerns about the flow-induced vibration, these vortices might cause, and about their effects on pump performance, led to conduct of a follow-up basic study in the 1:10-scale sump model, which had its goal elucidation of the processes responsible for vortex formation in pump suction bells and development of practical means of suppressing or at least attenuating these vortices. Before presenting the results of this basic study it is appropriate first to present as background material a general description of the Lake Chicot Pumping Plant and the flows in it which produced the suction-bell vortices.

The Lake Chicot Pumping Plant, which is located on the west-bank levee of the Mississippi River in Chicot County, Arkansas, is being constructed to divert flood waters approaching Lake Chicot directly into the Mississippi River, in order to reduce turbidity levels in Lake Chicot. The general layout of the plant is shown in figure 1-1; the plant* includes 12 pump bays and 3 gravity-flow bays. During periods of high Mississippi River stages the diverted flow will be pumped, while during low river stages it will pass through the gravity-flow sections. Twelve pumps, consisting of ten identical pumps rated at 600 cfs each and two identical units rated at 250 cfs each, will pump up to 6,500 cfs against a pool-to-pool head of up to 17.7 ft. Each pump bay is 23 ft wide. Three gravity-flow sections, each 26 ft wide, will be located at the center of the structure. The layout is

* A detailed plan and sections are presented in the Appendices.

symmetrical about the center gravity-flow bay, with the 250-cfs pumps adjacent to the gravity-flow section.

The study utilizing the 1:24-scale laboratory model of the complete plant, shown in figure 1-1 (Nakato and Kennedy 1976), demonstrated that during pump operation the forebay flows approaching the closed gravity-flow bays are diverted laterally and enter the pump bays with a strong transverse component of velocity. The abrupt redirection of the flows at the entrances to the pump bays led to separation which produced a large captive eddy and strong lateral nonuniformity in the distribution of velocity in the pump-approach flow in each pump bay. To reduce these lateral velocity nonuniformities to an acceptable level, modified trash racks with deep vertical bars* were proposed. These served, in effect, as turning vanes and were found to be surprisingly effective in producing uniformly distributed pump-approach flows. However, some concern arose about possible Reynolds-number scale effects in the 1:24-scale model screens. To resolve these doubts, a single, idealized, 1:10-scale model sump was constructed in one wall of the uniform approach channel of the 1:24-scale model. An identical idealized sump, but with a scale of 1:24, was placed in the other wall of the approach channel. A plan view and section details of the 1:10-scale sump model are shown in figures 1-2 through 1-4. Pairs of tests were conducted in these two idealized sump models, in order to determine the significance of scale effects. None were found.

However, during the tests with the 1:10-scale sump model, strong vortices were discovered extending from the sump floor and/or walls into the suction bell (Nakato and Kennedy 1976). Recent prototype experience has demonstrated that these vortices can produce undesirable and even damaging vibration problems, presumably by the nonuniform hydrodynamic loading they produce around the pump impellers (EDF 1967). Because of the large size of the prototype impellers and the severe pump-approach flow conditions, it was judged prudent to carry out further studies, which would be more basic in nature, on the characteristics of these vortices and means for supressing them. This basic study is reported herein.

---

* Trash-rack bars are placed on an inclined plane (see figure 1-3).

The primary objective of the investigation was to develop sump configurations which would improve the distribution of flows to, around, and into pump suction bells. A second objective was to find a means of eliminating, or largely suppressing, concentrated vortices which extend from suction bells to the sump floor or walls. A final objective was to investigate further the effects of trash-rack depth on the pump-approach flow distributions, and in particular to find the optimum depth for the bars of the proposed modified trash racks.

At the outset it is perhaps useful to review certain general considerations related to vorticity in fluid flows. Vorticity is the hydrodynamic term referring to the rotation of a fluid due to the gradients (i.e., spacial derivatives) of velocity. As a fluid element moves, the angular momentum corresponding to its vorticity is preserved unless the fluid is acted upon by a torque which opposes the fluid motion. Thus, for example, as a swirling fluid passes through an axisymmetric contraction in a circular pipe, the swirling, or angular velocity, of the fluid is intensified. The situation is precisely analogous to an ice skater who increases his rate of spin by pulling his extended arms inward. It can be demonstrated that the product of vorticity in any direction multiplied by the cross sectional area perpendicular to the component of vorticity of flow along a stream tube or a filament is constant; a discussion of this and of Helmholtz's equations for vorticity can be found in most upper level hydrodynamics texts. In the case of flows passing from pump bays through suction bells and into pumps, any vorticity (i.e, rotation) in the flow in the pump bay can be expected to produce progressively higher fluid angular velocities as the flow converges. Now it is well known that the pressure decreases toward the center of a vortex. If a vortex is sufficiently intense, the pressure at its center will drop to a point that dissolved gas will be brought out of solution in the liquid and concentrated at the vortex core, thereby making it visible. Moreover, the low density of the gas compared to the liquid will cause the gas to remain concentrated at the vortex core. It is in this way that the cores of sufficiently intense line vortices are made visible by the gas brought out of solution and held there. Note that the absence of the appear-

ance of free gas at the vortex core does not mean that no vortexing is occurring; it merely indicates that any vortex action which is present is not sufficiently strong to bring visible concentrations of gas out of solution in the liquid.

II. THE MODEL

A. Model Characteristics. The model utilized in the present study was essentially the same as that described by Nakato and Kennedy (1976). The 1:10-scale model was modified somewhat, in order to achieve test conditions consistent with the program objectives. The principal modifications were as follows:

1. Improvement of the inflow condition for the 1:10-scale sump. In the idealized 1:10-scale model the primary forebay flow was perpendicular to the sump axis. Accordingly, this model sump experienced a more severe inflow condition than the prototype sumps. For this reason, a training wall was installed which produced a pump-approach-flow velocity distributions in the idealized model which nearly duplicated the worst ones observed in the tests in the 1:24-scale model of the full plant. The training-wall configuration utilized was arrived at by repeated testing; it is shown in figure 2-1. It also can be seen in the photograph in figure 2-2, which presents a general view of the idealized 1:10-scale model sump.

2. Installation of transparent components. To facilitate flow visualization in the model, the cone-shaped suction bell, straight portion of the model siphon line, sump ceiling, and one pump-sump wall were removed and replaced by lucite components. These can be seen in the photograph presented in figure 2-2.

3. Vortimeter. The four-vane vortimeter mounted on a shaft supported by a low friction, stainless steel bearing was installed in the straight portion of the siphon-line (I.D. = 10 in.), just above the top of a cone-shaped suction bell. The vortimeter was used to obtain a measure of the net hydrodynamic circulation in the pump-approach flow. The vortimeter can be seen in figure 2-3.

4. Installation of false floor and pressure transducers. A portion of the concrete floor of the 1:10-scale model originally utilized was removed and replaced by a false floor fabricated from 1/4-in. thick aluminum plate and fitted with five strain-gage pressure transducers positioned as shown in figure 2-4.

B. Experimental Equipment. The following instrumentation, which is described in detail by Nakato and Kennedy (1976), was used in the present investigation:

1. Discharges in the model were measured by means of calibrated orifice meters and two-tube vernier-gaged manometers.
2. Water surface elevations were measured using conventional point gauges.
3. Velocities were measured with a miniature current meter manufactured by Novar Electronics of Great Britain (type 403).
4. Net flow circulation was measured by means of the aforementioned vortimeter.
5. Pressure fluctuations on the sump floor were measured with the pressure transducers (Endevco, Model PM131C, sensing area = 1/2-in. in diameter) connected to an amplifier (Preston, Model A, Type P/N 62060) and a balancing circuit. A calibration of the transducer was made *in situ* against static pressures in the model sump. A typical calibration curve for channel 1 is shown in figure 2-5. The calibration constant for each channel was as follows:

Channel 1: 0.745 ft (H_2O)/Volt
Channel 2: 0.775 ft (H_2O)/Volt
Channel 3: 0.680 ft (H_2O)/Volt
Channel 4: 0.802 ft (H_2O)/Volt
Channel 5: 0.758 ft (H_2O)/Volt

6. Flow visualization of sump-flow patterns and/or vortex activity around the suction bell was accomplished by means of floating confetti or with food dye injected from a dye reservoir through a long tube tipped with hypodermic tubing.

III. PRESENTATION OF EXPERIMENTAL RESULTS

The conditions under which model tests were performed and the principal results are summarized in table 1. Note that prototype values of sump elevations, flow rates, trash-rack dimensions, and sump backwall shift are presented therein. A step-by-step approach was utilized in the model test to arrive at the optimal sump configuration, with backwall position, sidewall convergence, and splitter-plate geometry being optimized in turn Accordingly, the test results from each step will be described *en suite* in the following.

A. Inlet Adjustment. It was desired in the 1:10-scale sump test to have an inlet-flow condition which reproduced one of the most severe ones observed in the test on the 1:24-scale model of the complete plant layout. Accordingly, a training-wall configuration was arrived at by trial and error, which reproduced the inlet-flow distribution in sump 5(a 600-cfs unit nearest the gravity flow sections) for the condition of all twelve pumps operating at a rated discharge. The training-wall configuration arrived at is shown in figure 2-1, and the inlet velocity profiles measured in the 1:10-scale and 1:24-scale sumps are shown in figure 3-1. These velocity distributions were measured at a cross section 52 ft downstream from the pier noses with no trash racks installed, with a forebay elevation of 110 ft and a pump discharge of 660 cfs, which is 110% of rated capacity. Note that y_p and V_p denote, respectively, the prototype distance below the water surface and the prototype velocity. The conformity between the velocity distributions measured in the two different sumps is wholly satisfactory. In order to obtain, this well simulated approach-flow condition a prototype discharge of 990 cfs was passed down the forebay approach channel, and one-third of this discharge (330cfs) was allowed to pass the idealized sump and was discharged out of the model through the gravity flow sections. All tests results for the 1:10-scale model reported hereinafter were obtained using this simulated approach-flow condition, a pump discharge of 660 cfs, and a sump elevation of 110 ft, unless otherwise stated. Note also that all velocities reported hereinafter were measured at the cross section 52 ft downstream from the pier noses.

B. Tests Results Obtained with Original Sump Configuration. Test results obtained from the sump configuration originally proposed by Stanley Consultants and described by Nakato and Kennedy (1976) first will be presented, in order to provide base-line data against which flow distributions obtained with modified sump configurations can be judged.

The velocity distributions measured in the sump for Run E1 (no trash rack present) and Run E2 (1.5-in. deep trash rack installed) are depicted for comparison in figure 3-2. This trash rack had 1.5-in. deep vertical bars on 6-in. centers, and is the design originally proposed by Stanley Consultants; it will be referred to hereinafter as the standard trash rack. Figure 3-2 demonstrates that the pump-approach flow in Run E1 was strongly nonuniform, and was not significantly improved by the standard trash rack, which had vertical bars that were not sufficiently deep to extract a significant portion of the lateral momentum of the flow entering the pump bay from the forebay. The nonuniform flow distribution was a manifestation of the relatively intense vorticity in the approach flow in the pump sump. This vorticity persisted and was concentrated when the flow was accelerated into the suction bell and passed through the siphon line. The high degree of nonuniformity in the distribution of the approach flow was reflected, accordingly, in the large values of vortimeter frequency, ω_p, measured in Run E1 (ω_p = 11.9 rpm). The standard trash rack, which accomplished little in improving the uniformity of the flow distribution, also produced an almost insignificant reduction in the vortimeter frequency (Run E2).

Pressure fluctuations on the sump floor were measured by means of the pressure transducers described in Chaper II. The analog output from the transducer amplifier was displayed and photographed on an oscilloscope screen. The maximum pressure fluctuations (peak-to-peak amplitude) then were determined directly from the photographs. The pressure-record data included in table 1 were obtained from oscilloscope displays which covered a model time period of 50 sec. Figure 3-3 presents oscilloscope photographs of pressure fluctuation records obtained in Run E1 at the five floor positions shown in figure 2-4. It is seen in figure 3-3 that the floor experienced major pressure fluctuations, especially at the positions measured by channels 3 and 5;

at these locations the maximum fluctuations, H_p, were 15.7 ft and 4.6 ft (prototype dimension) of water, respectively. Note, however, that the floor pressure never became negative (relative to atmospheric pressure). The sudden pressure drops depicted in figure 3-3 were produced by the passage of intense, concentrated, gas-filled vortices across or near the transducers. The motion of the vortices was observed to be quite random in nature. Figure 3-4 presents photographs of typical floor vortices which extended from the suction bell to the sump floor. The vortices were made visible by the air or other gas brought out of solution and concentrated at the vortex core by the low pressures occurring there. These photographs were made prior to installation of the previously described false floor, with test conditions equivalent to those of Run E1. Figure 3-5 presents close-up photographs of vortices which were produced under this flow condition, and illustrates the concentric motion of the fluid surrounding the vortex core. Table 1 identifies the tests in which visible suction-bell vortices formed. It is also seen in table 1 that the pressure fluctuations for the run with standard trash rack (Run E2) were comparable to those measured in Run E1. However, the maximum pressure fluctuations were reduced significantly when the 12-in. deep trash rack, with vertical bars on 6-in. centers, was installed (Run E3); in this case H_p measured by channel 3 was reduced to 9.5 ft. Moreover, the vortimeter frequency, ω_p, was reduced by approximately 40% below that of Run E1. The reductions in H_p and ω_p both result from the improved uniformity of the pump-approach flow, and the corresponding reduction in the rate of vorticity transport to the suction bell.

C. Determination of Backwall Position. Installation of the 12-in. deep trash rack produced significant improvement in the distribution of pump-approach flow (Nakato and Kennedy 1976), and corresponding attenuation of the pressure fluctuations and reduction of the suction-bell vortices and circulation in the flow withdrawn through the pump-model siphon line. It was judged impractical to obtain further improvement in the pump-approach flow distribution by utilization of still deeper trash racks. Accordingly, the next step in the optimization testing was to seek a pump-sump layout which produced further attenuation of the vorticity flux to the suction bell. The first step was to reduce the clearance between the downstream edge of the suction bell and the sump backwall, to reduce the size of the zone of inten-

sely eddying fluid motion which formed there. In the originally proposed sump design the backwall was positioned 3 ft from the rear edge of the suction bell. It was observed in the course of the flow visualization tests that the fluid in the space between the backwall and the nearest lip of the suction bell was subjected to intense swirling, which served as a constant source of vorticity to the flow entering the suction bell.

In these tests a movable backwall was positioned at successively smaller distances from the suction bell until an optimum location, judged from the formation of visible suction-bell vortices and measured vortimeter frequencies, would be achieved. Run E4 was conducted with the backwall shifted forward by 6 in. (prototype dimension); the vortimeter frequency was found to be slightly higher than that of Run E2, and the maximum pressure fluctuation measured by channel 3 also was increased above that of Run E2. When the backwall was shifted forward an additional 6-in., for Run E5, the peak pressure fluctuation and the vortimeter frequency were roughly the same as those of Run E2, and no significant improvement in the pump-approach flow or vortex formation was observed during the flow-visualization test. However, when the backwall was shifted an additional 6-in., to give a total forward shift of 18 in. (Run E6), the vortimeter frequency was reduced to approximately 17% below that of Run E2, and the maximum pressure fluctuation also was decreased. Use of the 12-in. deep trash rack with the 18-in. forward shift of the backwall produced further improvement in the flow condition (compare Runs E6' and E2).

It then was expected that further reduction in the clearance behind the suction bell might produce additional improvement. Accordingly, Run E7 was conducted with a backwall shift of 24 in. and the standard trash rack. It is seen in table 1 that ω_p was reduced to less than half of the value obtained in Run E2, while H_p for channel 3 was reduced to less than 1/3 of its value of Run E2. It was observed, however, that with this backwall configuration, the point of attachment of the suction-bell vortices moved downstream, away from the floor pressure transducers and toward the backwall, and actually was some distance removed from the transducer of channel 3. Accordingly, it was judged that much of the reduction in the measured H_p was a consequence of the increased distance between the point of vortex attachment and

the pressure transducers. Indeed, visual observation of the floor vortex in Run E7 indicated that it might be stronger than the vortex which formed in the runs with larger backwall spacing. This points up one of the difficulties encountered in making boundary-pressure measurements with fixed transducers; the point of measurement cannot easily be shifted to the immediate vicinity of vortex attachment. It also highlights the importance of having boundary-pressure measurements accompanied by flow visualization tests. Figure 3-6 presents photographs of the suction-bell vortices which formed during Runs E2 and E7. The rearward shift of the vortex in Run E7 is clearly evident. It is also seen that the Run E7 vortex has a significantly larger core diameter. Note again the intense swirling fluid motion around the gas-filled core of the vortex in Run E2. A comparison of the pressure records obtained from channel 3 in Runs E4,E6, and E7 showed that both the amplitude and the frequency of the pressure fluctuations were considerably reduced in Run E6. The pressure records for Run E7 gave the impression of small fluctuations, but the reduction was believed to be due primarily to the shift of the point of floor attachment of the vortex away from the transducer, as discussed above. Flow visualization indicated that the flow approaching the suction bell in Run E7 was not better than that of Run E6, despite the reduction of ω_p in Run E7. It was judged, therefore, that, on balance, an 18-in. forward shift of the sump backwall was optimal.

D. Sidewall Contraction. One of the sources of vorticity in the flow entering the suction bells is the boundary layers which form along the sump floor and sidewalls. The boundary layer development is suppressed by a favorable pressure gradient, which can be produced by converging sidewalls. In an attempt further to reduce the vorticity flux into the suction bells, and thereby reduce the intensity of the suction-bell vortices, tests were made with converging sump sidewalls. All of these tests were conducted with an 18-in. forward shift of the backwall.

Four different sidewall convergences were tested; their configurations and prototype dimensions are summarized in figures 3-7. Fillets of type A (identified in figure 3-7) were tested in Run E8, and resulted in a significant reduction in vortimeter frequency below that measured in Run E6. The maximum pressure fluctuations recorded through channel 3 also were very low. However,

the region of floor attachment of the suction-bell vortex was observed to be shifted toward the backwall, and to be some distance away from the pressure transducers. It is believed that much of the reduction in the pressure fluctuation resulted from this shift.

Run E9 was conducted with type B fillets, which produced a less severe contraction than those of type A. A comparison of the results from Runs E8,E9, and E9' indicate that the type B fillets did achieve further reduction of the intensity of flow swirling in the flows entering the suction bell. Fillets of type C were tested in Run E10. Although the vortimeter frequency was slightly increased above that of Run E9, the vortex strength and the frequency with which it became severe enough to be visible were observed to be reduced significantly. Further upstream extension of the fillets would have reduced the rate of contraction, and therefore would have favored boundary-layer development. It was concluded that, on balance, fillets of type C produced the best pump-approach flow. The two small fillets, identified as type D in figure 3-7, will be discussed in the following section. Velocity distributions for Runs E9 and E10 are presented in figure 3-8. A comparison of these velocity distributions with those for Run E2, presented in figure 3-2, indicates that the sidewall contraction of the pump-sump is not effecting a significant improvement in the flow distribution.

E. Splitter Plates. Although the strength of the net circulation in the flow into the suction bell and pump siphon line, and the pressure fluctuations at the locations of the transducers on the sump floor were significantly reduced by the forward shift of the sump backwall and the convergence of the sump sidewalls, visual inspection during the flow-visualization tests indicated that the suction-bell vortices still were undesirably strong. As discussed above, these vortices result from the net rotation (i.e., the net vorticity) in the approach flow being concentrated as the flow passes through the suction bell and enters the siphon line. After the practical means for suppressing the vorticity in the approach flow had been exhausted, the next step in the program to reduce or eliminate the suction-bell vortices involved measures which would directly oppose the swirl by applying an opposing torque to the flow. Toward this end, vertical flow-splitter plates aligned with the sump were attached to the sump floor beneath the suction bell.

The initial tests in this phase of the investigation consisted of

a series of runs which were conducted to determine the optimum length and position of a single splitter plate. The results of these tests showed that a plate extending upstream from the sump backwall to the forward (upstream) lip of the suction bell yields the best pump-approach flow. Therefore, the further tests in this phase of the program were conducted with plates with this length and position, and three different heights. The dimensions and configurations of the splitter plates tested are shown in figure 3-9. Note that all splitter-plate tests were conducted in a converging sump of type C with the optimized backwall location, and that the splitter-plate thickness was the same in all tests.

The splitter plate of type A (see figure 3-9), which was tested in Run E11, was found to improve the suction-bell inflow pattern significantly, reduce the vortimeter frequency to a relatively low level, and suppress the pressure fluctuations until even their peaks were comparable with the static pressure changes due to water-surface fluctuations in the pump sump. Figure 3-10 presents photographs of the outputs of the five pressure transducers; a comparison of these photos with those presented in figure 3-3 illustrates the dramatic reduction in the floor-pressure fluctuations which was achieved by the step-by-step modification of the pump sump.

Run E12 was conducted with corner fillets of type D (see figure 3-7) in addition to the type C fillets, in an attempt further to reduce the vortimeter frequency by eliminating the corner areas which were occupied by fluid with no translational motion but intense swirling. However, the small corner fillets produced no measurable or observable improvement in the flow (compare Runs E11 and E12 in table 1). When the plate height was reduced by half (type B; see figure 3-9) for Run E13, the vortimeter frequency was roughly double that measured in Run E12.

The next test, Run E14, was conducted with the type C splitter plate; this has a height of 3.75 ft, which amounts to three-quarters of the clearance between the suction bell and sump floor. The vortimeter frequency was found to be only 1.3 rpm, significantly below that obtained with the lower splitter plates. Some very weak swirling activity was observed in the vicinity of the floor on each side of the splitter plate; this was eliminated by the wing walls which intersected the main splitter plate perpendicularly at the projection of the suction-line axis (type C' splitter plate). In Run

El5, however, a pair of strong, gas-filled vortices with horizontal axes were found to extend periodically from the sump backwall into the suction bell; one vortex occured on each side of the main splitter plate. These vortices apparently originated from the vorticity present in the flow along the floor to and up the main splitter plate. After the discovery of these backwall vortices, the type A' splitter plate again was installed in the model and additional detailed flow visualization tests were made by injecting dye successively at many different locations in the flow field. No backwall attached vortices were discovered with the type A' splitter plate. It then was concluded that the type A' splitter plate which produced a flow in which no persistent discernable eddies ever were observed to form, gave the best overall performance in suppressing section-bell vortices.

F. Modified Trash Racks. Preceding sections have described three different types of sump modifications which suppressed formation of suction-bell vortices, reduced the net hydrodynamic circulation in the suction-line flow, and minimized sump-floor pressure fluctuations. However, none of these modifications treats the principal origin of the vortex and pressure-fluctuation problem: the strong lateral nonuniformity of the pump-approach flow in the sump, which results from the large component of lateral velocity in the forebay just outside the pump sumps. As was discussed in some detail in Chapter I, the plant layout is such that when the gravity bays are closed and the pumps are in operation, the flow approaching the plant through the forebay is diverted laterally and, upon being redirected into the pump sumps, forms a strong captive eddy on the downstream side of each pier nose which gives strong velocity gradients across the sumps. Both the velocity gradients and the captive eddies serve as continuous sources of vorticity to the pump-approach flows in the sumps.

The effectiveness of modified trash racks, with 12-in. deep, 1-in. thick bars on 6-in. centers, in extracting much of the transverse momentum from the flow entering each pump sump was demonstrated in the earlier model tests reported by Nakato and Kennedy (1976). Additional trash-rack tests were undertaken in the investigation reported herein, in order to determine an optimum depth for the modified trash racks. In most of the tests reported above, to determine the effects of backwall spacing, sidewall convergence, and splitter plates on the formation and persistence of suction-bell

vortices, the standard trash racks, with 1.5-in. deep bars were used. The earlier model tests by Nakato and Kennedy (1976) demonstrated that the standard trash racks produced pump-approach flows in the sumps which had an unacceptably high degree of lateral nonuniformity. As can be seen in figures 3-2 and 3-8, these trash racks had little effect on the velocity distributions in the pump sumps. Figures 3-11, 3-12, and 3-13 show the vertical distributions of sump velocity measured in Runs E15' (with a 12-in. deep trash rack), E15" (with a 9-in. deep trash rack), and E15"' (with a 6-in. deep trash rack), respectively. Each test was conducted with a water-surface elevation of 110 ft and a pump discharge of 660 cfs. In all three of these trash racks the vertical bars were spaced on 6-in. centers. A comparison of these figures indicates that a 9-in. deep trash-rack is most effective in reducing the lateral nonuniformity of the velocity distribution (see figure 3-2 for comparison). The data presented in table 1 for Run E15" show that the vortimeter frequency was practically zero when this trash rack was installed in a fully modified sump. Sump velocity distributions downstream from the 12-in. deep and 9-in. deep trash racks also were measured for a water-surface elevation of 108.5 ft (Runs E16 and E16'); the results are shown in figures 3-14 and 3-15, respectively. In these figures, 9-in. deep trash rack is seen to yield velocity distributions with a higher degree of lateral conformity. Note that the vertical distributions of velocity measured behind a trash rack with deeper bars are more nonuniform (see figures 3-11 through 3-15), especially in comparison to the profiles measured downstream from the 1.5-in. deep trash rack, shown in figures 3-2 and 3-8. The stronger vertical nonuniformity downstream from the deeper trash-rack bars is believed to result from preservation of the vertical gradient of velocity present in the approach flow in the forebay. If no trash rack, or only a shallow one, is present, separation occurs as the flow passes around each pier nose, and produces intense eddying, a high level of turbulence, rapid vertical exchange of horizontal momentum, and consequently a nearly uniform vertical distribution of velocity. If a deeper trash rack is installed, which acts as an effective turning-vane array, the production of large scale eddies and the accompanying intense vertical mixing is suppressed. Outside the pump bays, in the forebay, the approach flow has its highest velocity at or near the free surface and a monotonic negative velocity gradient toward the bed. If no large scale mixing produces vertical transport of horizontal momentum, this velocity

gradient can be expected to persist, although attenuated as the flow enters the pump bays.

Further trash-rack comparison tests were conducted with a pump discharge of 600 cfs (100% of rated capacity) at a water-surface elevation of 110 ft. The results are shown in figures 3-16 (Run E17) and 3-17 (Run E17') wherein the superior performance with a 9-in. deep trash racks again is demonstrated. Finally, tests were made at a water-surface elevation of 108.5 ft and a pump discharge of 600 cfs; the results are presented in figures 3-18, (Run E18) and 3-19 (Run E18') which lend further support to the conclusion that the 9-in. deep trash racks are preferable.

The tests conducted with the optimum sidewall convergence (type C), a type A' splitter plate, and the 9-in. deep trash rack produced a vortimeter frequency of less than 1 rmp (prototype) for discharges of 600 cfs and 660 cfs, and for the water-surface elevations of 108.5 ft and 110 ft (refer to the data for Runs E15", E16', E17', and E18' in table 1).

G. Baffle Blocks. The effectiveness of baffle blocks in reducing the lateral nonuniformity of the sump flows was tested by installing two staggered rows of 1.00-ft square blocks extending vertically above the water surface on the sloping section of the sump floor; the blocks were arrayed as shown in figure 3-20, with the forward faces of the upstream baffle blocks located 21 ft downstream from the pier noses. Also included in figure 3-20 are the velocity distributions measured in Run E20, which was made with the original rectangular sump configuration and the standard trash rack. A comparison of figures 3-2 and 3-20 demonstrates that the baffle blocks did produce significant improvement in the lateral uniformity of the sump flow. In the flow visualization tests, however, it was found that small vortices initiated in the wake of each baffle block tended to concentrate into larger, persistent, water-surface-attached eddies immediately upstream from the vertical wall which extends upward from the pump ceiling (refer to figure 1-3). These surface-attached eddies were made readily apparent by the depression where they intersected the water surface, and often were sufficiently strong to draw confetti sprinkled on the water surface into the suction bell. Vortices extending from the sump floor into the suction-bell were observed in Runs E20 and E20' despite the improved distribution of the pump-approach flow because no splitter plate was installed. Runs E19

and E19' were conducted with type C converging sidewalls and type C' splitter plate. In both of these tests relatively low vortimeter frequencies and floor-pressure fluctuations were measured. However, small swirling eddies, resulting from concentration and organization of the vortices shed from the baffle blocks, which were similar to those observed in Runs E20 and E20', again were noted. Because the primary reason for attempting to minimize vortex activity in the sump flows was to minimize the strength of vortices extending into the suction bells and suction lines, utilization of baffle blocks in relatively short pump sumps does not appear to be attractive.

The vertical uniformity of velocity distributions shown in figure 3-20 is striking. It is believed to be a consequence of the intense vertical mixing produced by the turbulence generated by the baffle blocks, which completely suppress the vertical gradients of streamwise velocity in the flow reaching the baffle blocks from the forebay.

H. Forebay Flow Patterns With Extended Gravity-Bay Piers. In a further attempt to improve the overall forebay flow patterns, a series of tests was conducted in the 1:24-scale model with the gravity-bay piers extended significantly upstream into the forebay. A total of four tests was carried out under one operating condition: all pumps, except the three nearest to the left bank plant, operating at 100% of the rated capacity (total discharge of 4,700 cfs), and a forebay water-surface elevation of 110 ft.

Velocity distributions first were measured in each operating pump bay with no modification to the gravity-bay piers. Note that no trash racks were installed, and that mean velocities were measured at five different positions across a section located 52 ft downstream from the pump pier noses. One velocity was measured on each vertical, at a distance below the water surface of 0.4d, where d is the local flow depth. The velocity measured at this elevation yields at least a rough measure of the vertically averaged velocity for each vertical. Figure 3-21 shows the velocity distributions measured with no gravity-bay pier extension. Nonuniform distributions of the pump-bay flows due to the presence of the gravity-flow sections in the center of the plant are evident. Flow separation from each pump-bay pier produced a captive eddy in the wake of each pier and produced strong lateral

velocity gradients. Indeed, at some locations close to the pier noses the pump-bay flows were away from the pump.

When the two outside gravity-bay piers were extended upstream 384 ft, the forebay flow was found to separate from the gravity-bay pier noses, thereby producing long captive eddies on each side of the extended piers. The general forebay flow pattern and the pump-bay flow distributions for this case are shown in figure 3-22. Because of the strong circulations set up by the extended piers, the transverse component of the inflows to pump bays 8 and 9 was reversed relative to that occuring without the pier extension (see figure 3-21). Figure 3-23 summarizes the test results obtained with a gravity-bay pier extension of 164 ft. The pump-bay flows are somewhat more uniform than those presented in figure 3-22 (384 ft pier extensions). The forebay flow, however, still separated from the gravity pier noses and set up a large scale circulation in the forebay segment in front of each of the two groups of pumps. Finally, the pier extension was further reduced to 96 ft, and the results summarized in figure 3-24 were obtained. A supplementary test in which the 9-in. deep trash rack was installed to verify its effectiveness in improving the pump-approach flows in the sumps, was conducted; the resulting velocity distribution in pump bay 8 is included in figure 3-24.

Extending the outside piers of the gravity-flow bays into the pump forebay does achieve some improvement in the lateral distribution of the depth-averaged velocity in each pump bay. However, the large scale eddies produced in the forebay at the extensions themselves produced transverse velocity components at the entrances to the pump bays which tended to have precisely the effect the extensions were intended to overcome.

IV. CONCLUSIONS AND RECOMMENDATIONS

The principal conclusions derived from this model investigation may be summarized as follows:

Reduction of the clear distance between the downstream lip of the suction bell and the backwall of the pump sump to 18-in. appears to be optimal in improving the configuration of the flow to, around, and into the suction bell. Convergence of the sump sidewalls was found to be quite

effective in reducing the intensity of the floor-attached vortex extending into the suction bell and, accordingly, in reducing the strength of the hydrodynamic circulation in the pump inflow. The sidewall constraction labeled type C and illustrated in figure 3-7 was found to be the best among those tested. Floor mounted splitter plates aligned with the sump axis and extending to the sump backwall are very effective in suppressing suction-bell vortices, suction-line circulation, and sump-floor pressure fluctuations. The splitter-plate configuration designated type A' and depicted in figure 3-9 was found to be most effective among the several tested in this program. Trash racks with 9-in. deep bars spaced on 6-in. centers produced pump-bay flows that were more uniformly distributed than those produced by the 6-in. and 12-in. deep trash racks tested. Baffle blocks installed in the pump bay improved the uniformity of the velocity distribution, but produced strong surface eddies which can become concentrated and serve as sources of additional vorticity in the flow entering pump. Extension of the outer piers of the gravity-flow bays into the forebay, in order to improve the alignment of the flow approaching the pump bays through the forebay, proved not to be effective. The forebay extensions themselves produced flow separation and large scale eddies which imparted lateral components of velocity to the flows entering the pump bays. The principal recommendations based on this investigation are as follows:

1. The backwalls of the pump sumps should be shifted upstream 18-in. from the location proposed in the original design.
2. The pump-sump sidewalls should converge, following the scheme identified as type C herein and illustrated in figure 3-7.
3. Splitter plates, type A' (see figure 3-9) should be installed in each pump bay.
4. Trash racks made up of 9-in. deep bars located on 6-in. centers should be installed.
5. The pump-sump ceilings, above the pump intakes, should be sloped upward in the upstream direction, to provide for escape of any air that becomes trapped in the pump sumps.

LIST OF REFERENCES

JULIO O. LOZOYA CORRALES, AND JORGE SALINAS ELORREAGA, "Estudio de un Modelo Hidraulico de la Planta de Bombeo-El Porvenir-en San Luis Potosi," Proceedings of 4th Congreso National de Hidraulica, Asociacion MEXICANA de Hidraulica, Paper No. 31, Oct., 1976.

EDF (Département Laboratoire National D'Hydraulique), "Centrale Thermique de NANTES-CHEVIRE," Etude Sur Modéle Réduit Des Ecoulements Aux Aspirations Des Pompes De Circulation, AV a/LV, HJ4/R/203, 15.1.1967.

FLETCHER, B.P., AND GRACE, J.L., JR., "Flow Conditions at Pumping Stations, Cairo, Illinois; Hydraulic Model Investigation," Technical Report H-77-3, Waterways Experiment Station, Vicksburg, Mississippi, March, 1977

NAKATO, T., AND KENNEDY, J.F., "Model Study of the Lake Chicot Pumping Plant," IIHR Report No. 188, Iowa Institute of Hydraulic Research, The University of Iowa, Iowa City, Iowa, August, 1976.

MICHAEL C. QUICK, "Efficiency of Air-Entraining Vortex Formation at Water Intake," Journal of the Hydraulic Division, ASCE, Vol. 96, No. HY7, Proc. Paper 7399, July, 1970.

PETER E SAUNDERS, "Pumping Stations For Drainage District No. 17, Mississippi County, Arkansas-Hydraulic Model Investigation," Technical Report H-77-12, Waterways Experiment Station, Vicksburg, Mississippi, May, 1977.

ZEIGLER, E.R., "Hydraulic Model Vortex Study-Grand Coulee Third Power Plant," Bureau of Reclamation Report REC-ERC-76-2, February, 1976.

Table 1. Test conditions and summary of results

Run No.	Sump El. (ft)*	Flow Disch. (cfs)*	Trash-Rack Depth (in.)*	Back-Wall Shift (in.)*	Fillet I.D.	Splitter Plate I.D.	Vortimeter Freq. ω_p (rpm)*	Max. Pressure Fluctuations H_p (ft in H_2O)* Chan. 1	Chan. 2	Chan. 3	Chan. 4	Chan. 5	Floor Vortex?
E1	110	660	No	No	No	No	11.9	0.8	1.2	15.7	1.0	4.6	Yes
E2	110	660	1.5	No	No	No	10.3	1.5	0.8	16.3	0.8	0.8	Yes
E3	110	660	12	No	No	No	6.8	0.2	0.8	9.5	0.2	0.2	Yes
E4	110	660	1.5	6	No	No	12.2	0.8	0.8	17.3	0.8	3.0	Yes
E5	110	660	1.5	12	No	No	10.4	0.7	0.8	17.0	0.8	6.8	Yes
E6	110	660	1.5	18	No	No	8.5	0.4	0.8	12.9	1.6	1.5	Yes
E6'	110	660	12	18	No	No	4.7	--	-	6.8	-	-	Yes
E7	110	660	1.5	24	No	No	4.8	0	0	4.8	0.8	0.8	Yes
E8	110	660	1.5	18	A	No	5.4	0	0.4	4.1	0.7	2.3	Yes
E9	110	660	1.5	18	B	No	4.5	0	0.4	2.7	3.2	3.8	Yes
E9'	110	660	12	18	B	No	3.7	-	-	1.0	0.8	0.8	Yes
E10	110	660	1.5	18	C	No	5.0	0	0	1.7	2.6	0.8	Yes
E10'	110	660	12	18	C	No	3.4	-	-	6.1	-	-	Yes
E11	110	660	1.5	18	C	A	2.2	0	0	0.3	0.4	0.4	No
E11'	110	660	12	18	C	A	1.5	-	-	0.3	-	-	No
E12	110	660	1.5	18	C&D	A	2.1	0	0	0.3	0	0	No
E12'	110	660	12	18	C&D	A	1.5	-	-	0.3	-	-	No
E13	110	660	1.5	18	C	B	4.6	0	0	0.3	0	0	No
E13'	110	660	12	18	C	B	2.7	-	-	0.3	-	-	No
E14	110	660	1.5	18	C	C	1.3	0	0	0.3	0	0	No
E14'	110	660	12	18	C	C	1.0	-	-	0.3	-	-	No
E15	110	660	1.5	18	C	C'	1.6	0	0	0	0	0	No
E15'	110	660	12	18	C	C'	0.9	-	-	0	-	-	No
E15"	110	660	9	18	C	A'	0	-	-	0	-	-	No
E15"'	110	660	6	18	C	C'	1.0	0	0	0	0	0	No
E16	108.5	660	12	18	C	A'	1.4	-	-	0	-	-	No
E16'	108.5	660	9	18	C	A'	1.0	-	-	0	-	-	No
E16"	108.5	660	6	18	C	A'	2.8	-	-	0	-	-	No
E17	110	600	12	18	C	A'	1.8	-	-	0	-	-	No
E17'	110	600	9	18	C	A'	0.4	-	-	0	-	-	No
E18	108.5	600	12	18	C	A'	1.0	-	-	0	-	-	No
E18'	108.5	600	9	18	C	A'	0.6	-	-	0	-	-	No
**E19	110	660	1.5	18	C	C'	1.5	0	0	0	0	0	No
**E19'	110	660	12	18	C	C'	0.8	-	-	0	-	-	No
**E20	110	660	1.5	18	No	No	0.9	0	0	1.4	1.4	0	Yes
**E20'	110	660	12	18	No	No	0	-	-	0.7	-	-	Yes

* Dimensions in prototype

** With baffle blocks

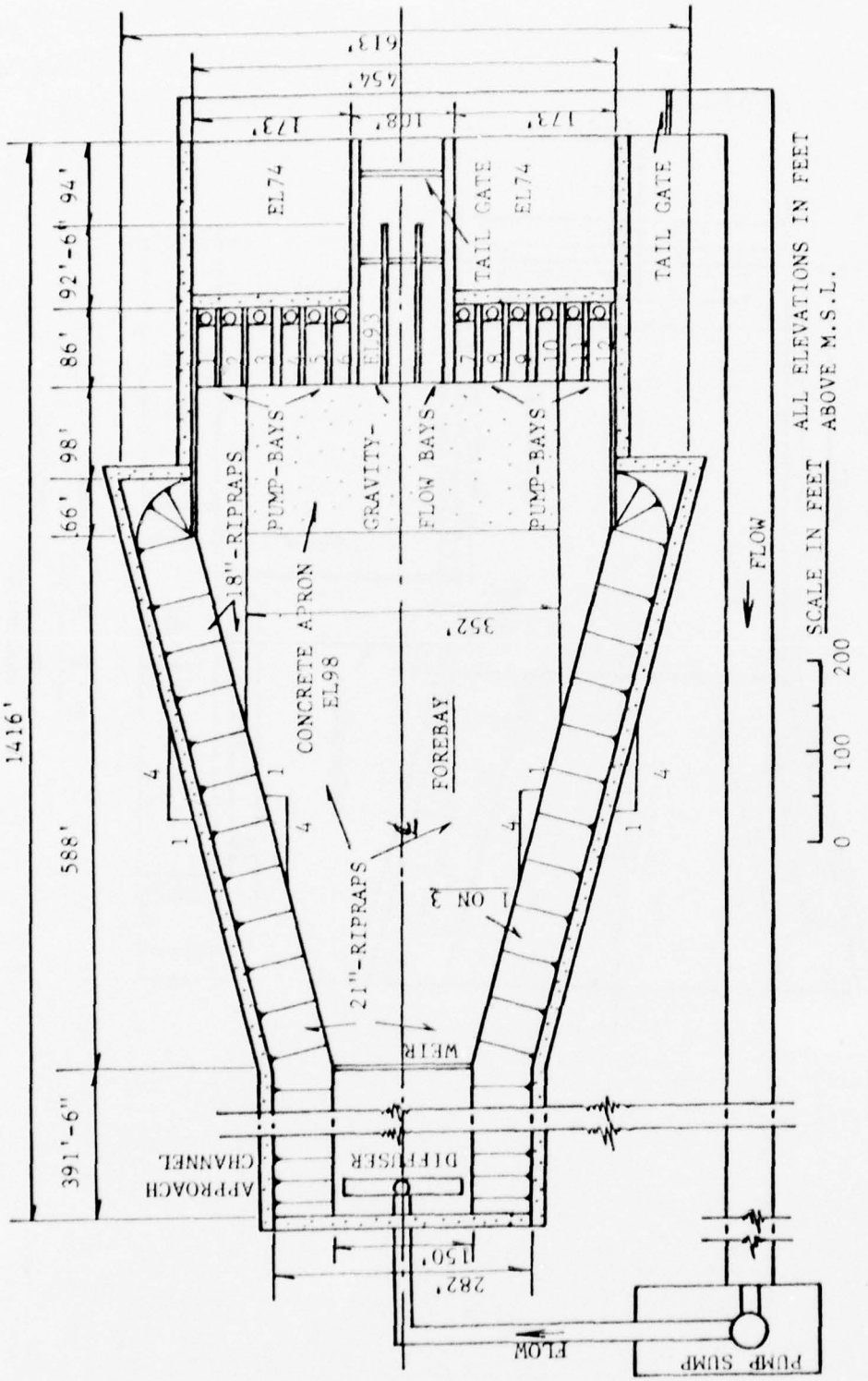

Figure 1-1. Schematic plan view of the Lake Chicot Pumping Plant model

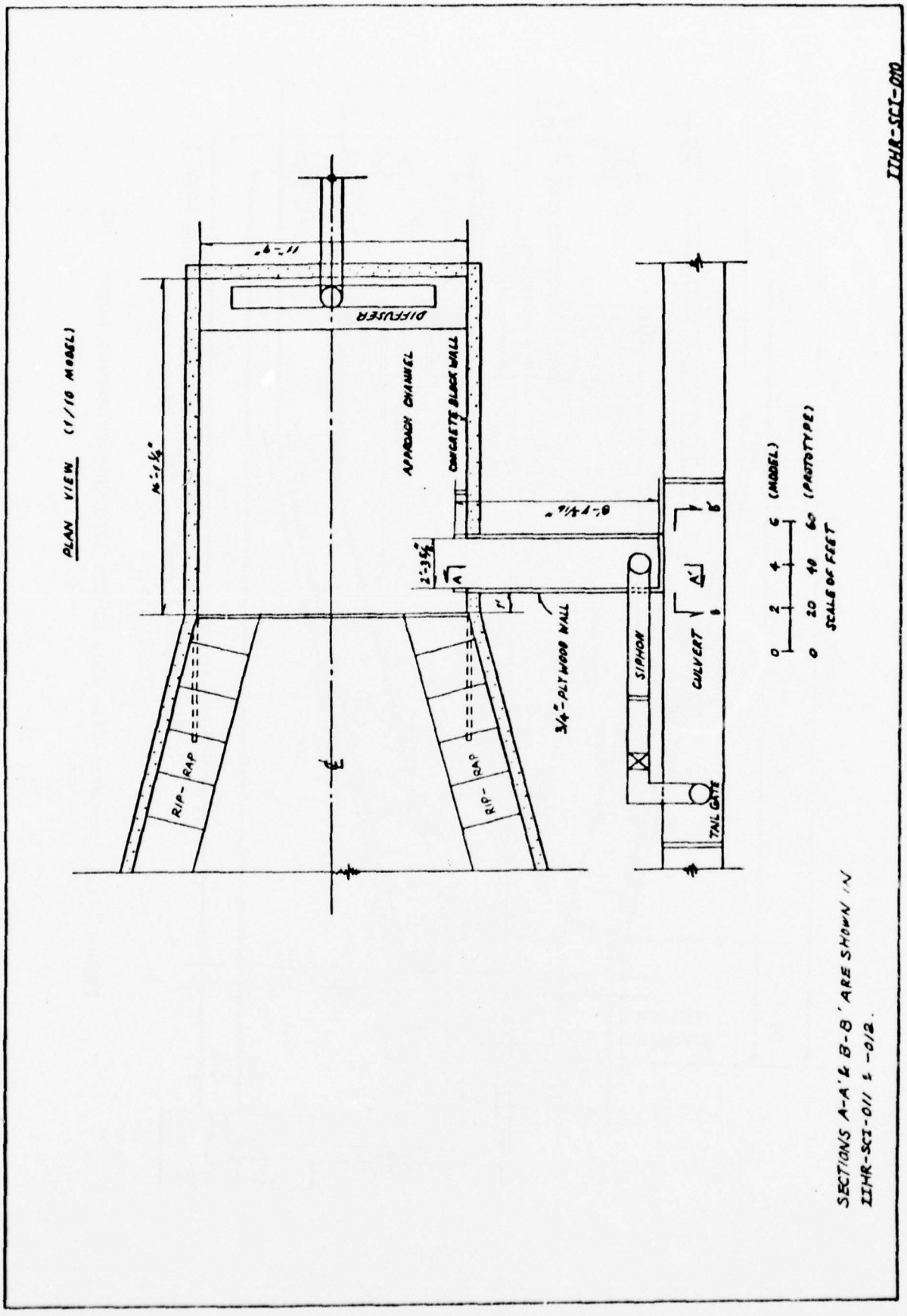

Figure 1-2. Plan view of 1:10-scale sump model

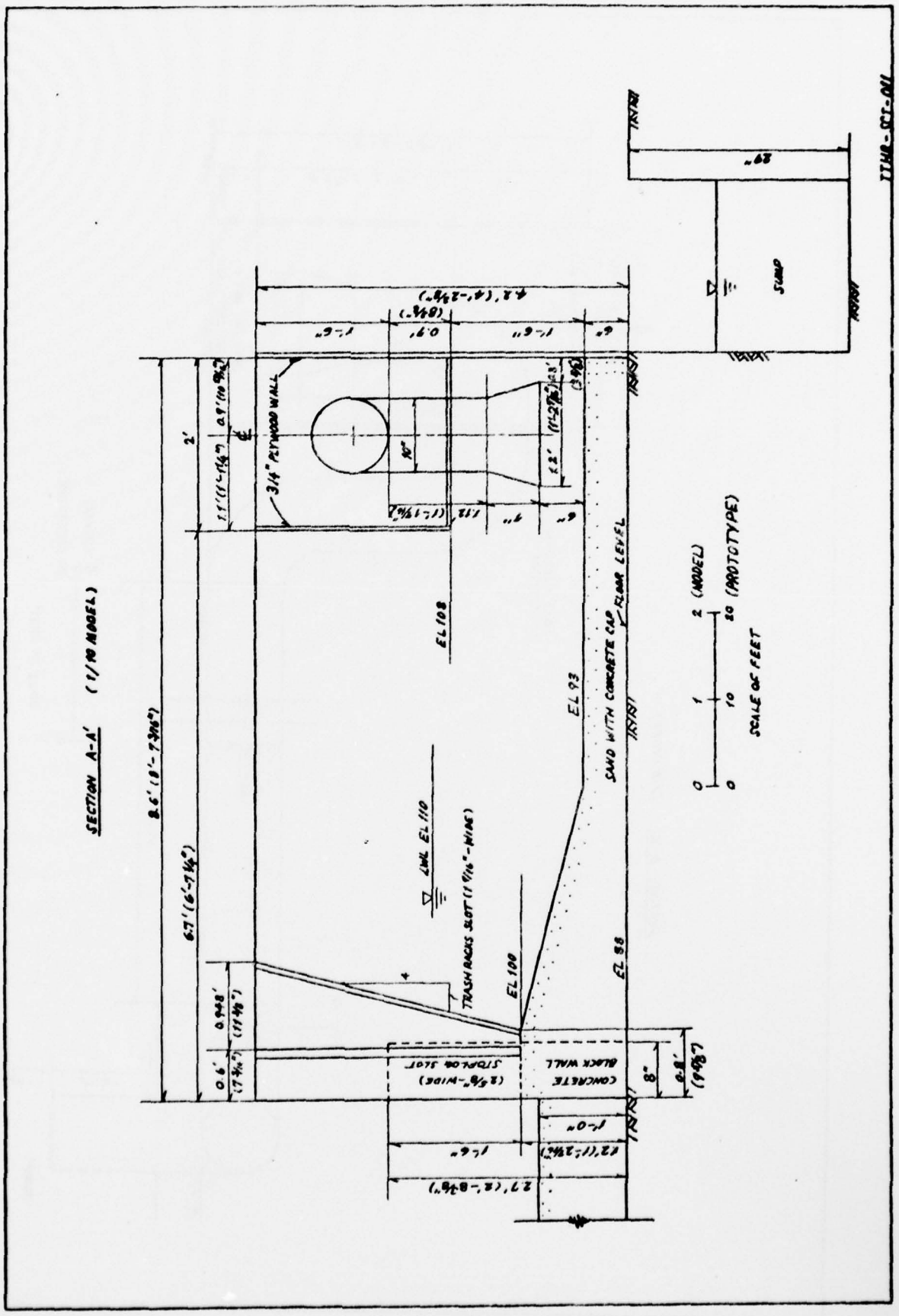

Figure 1-3. Section of 1:10-scale sump model

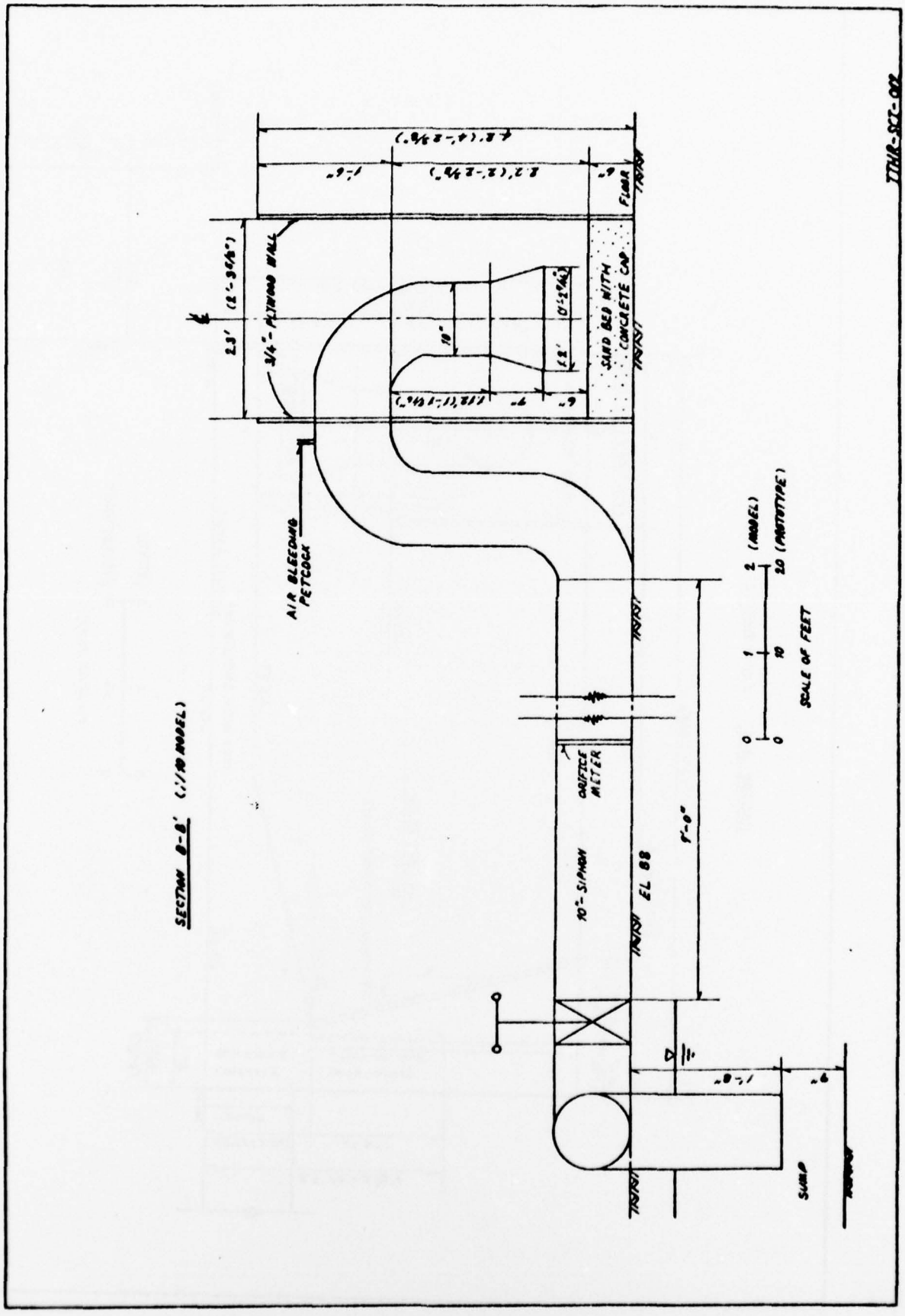

Figure 1-4. Section of siphon system for 1:10-scale sump model

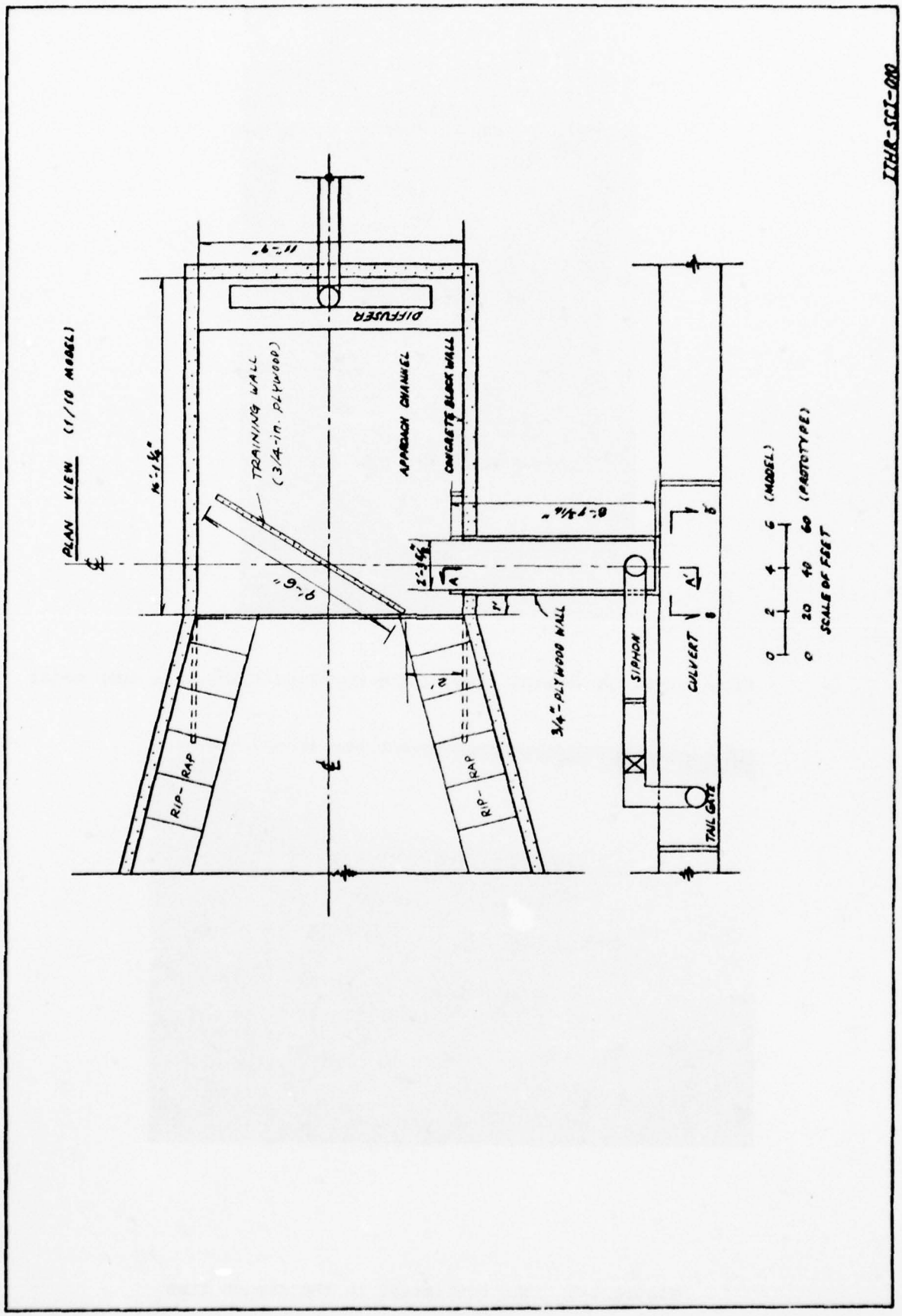

Figure 2-1. Location of the training wall in the forebay

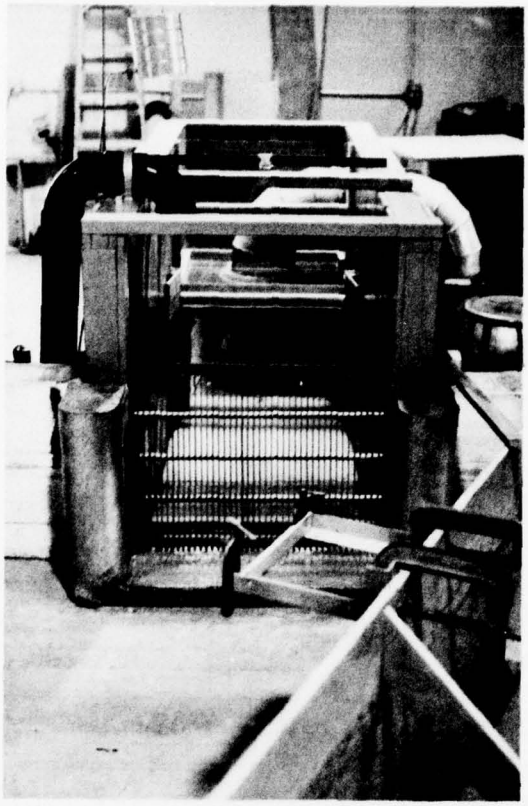

Figure 2-2. A general view of the modified 1:10-scale sump model

Figure 2-3. The vortimeter in the siphon line

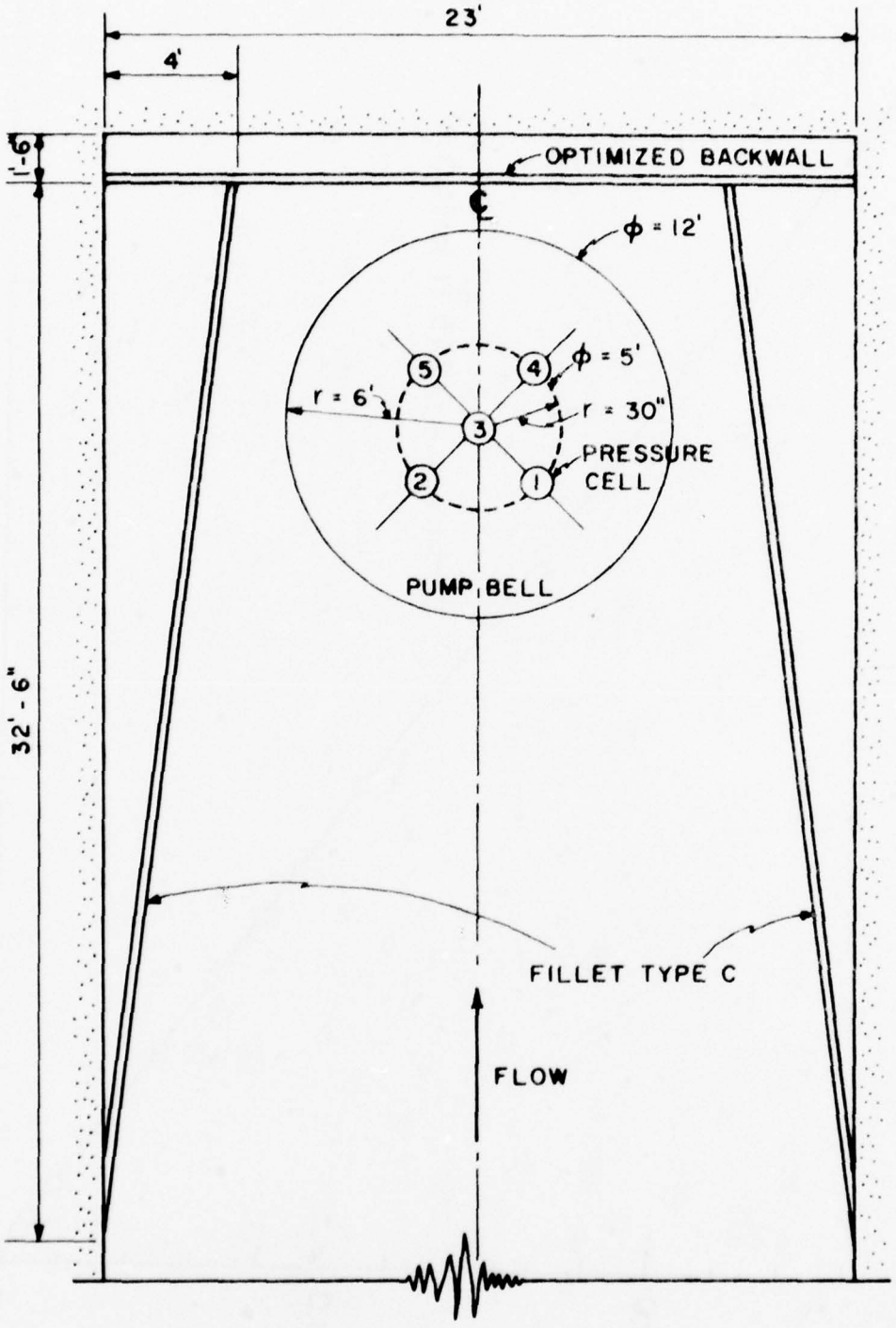

Figure 2-4. Locations of pressure transducers

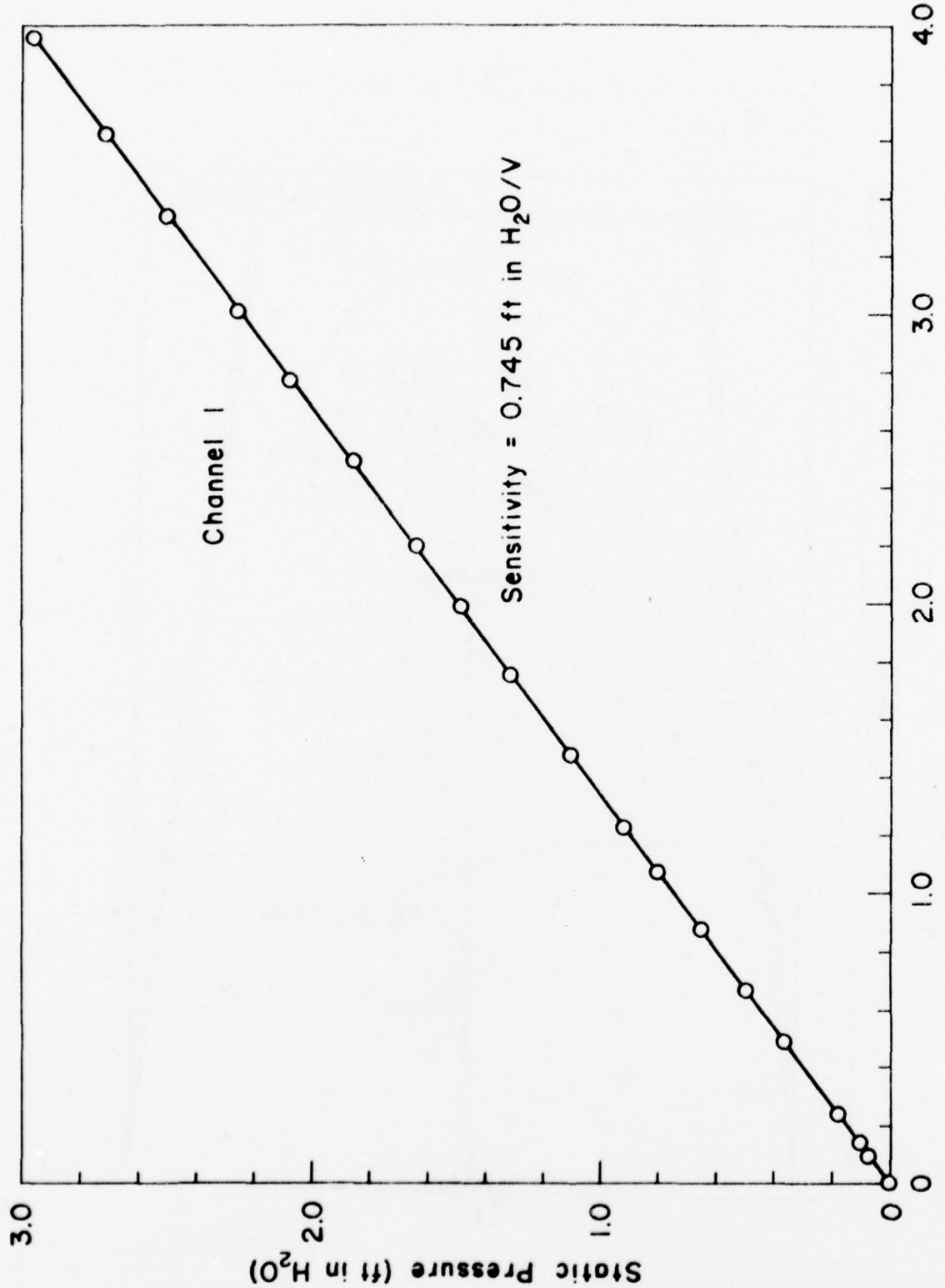

Figure 2-5. A typical calibration curve for pressure transducer

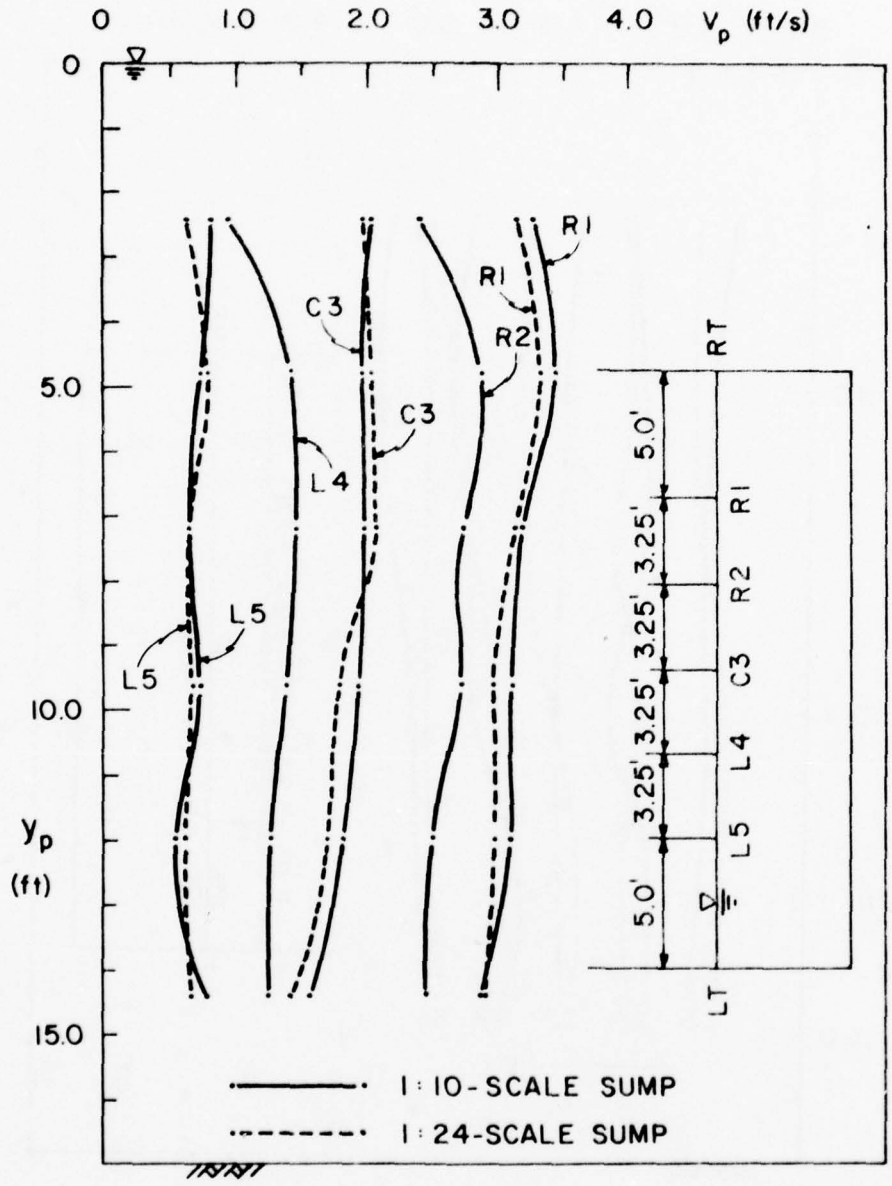

Figure 3-1. Velocity profiles obtained in both 1:10-scale and 1:24-scale models (no trash rack present, Q_p = 660 cfs, 110% operation)

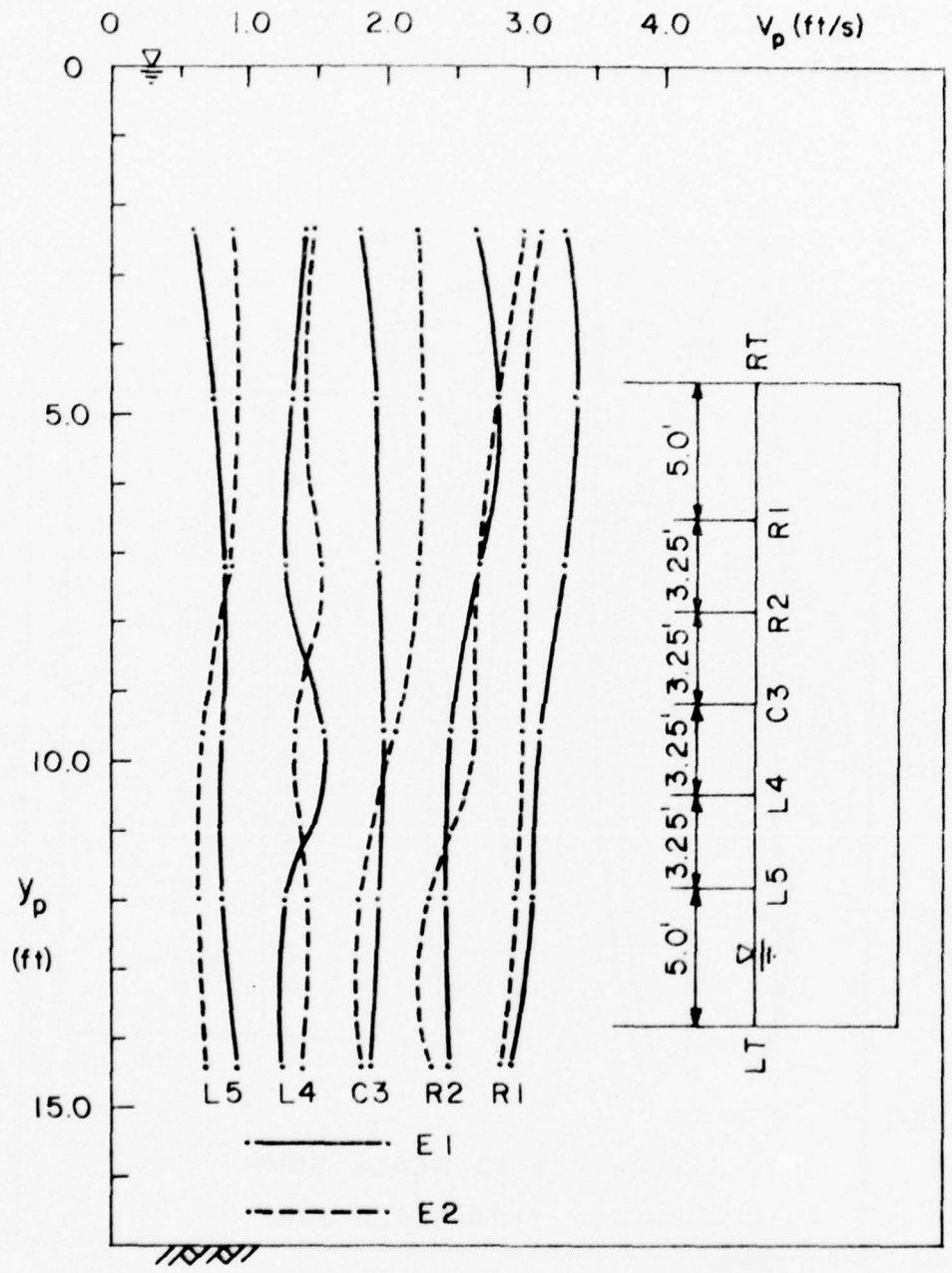

Figure 3-2. Velocity profiles obtained in Runs E1 and E2

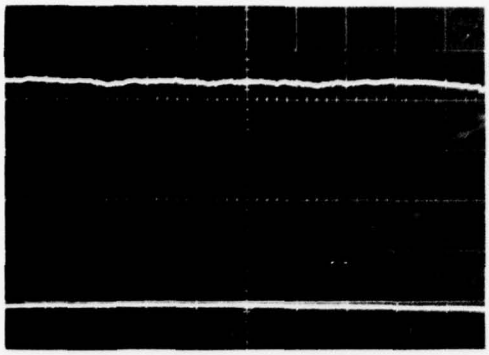

Channel 1

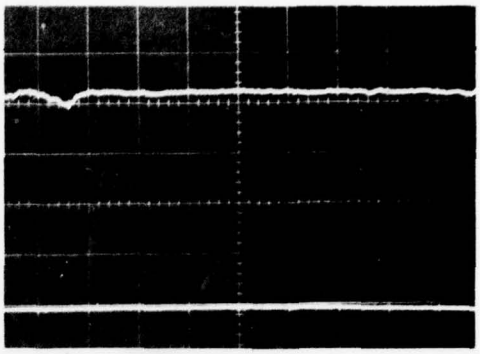

Channel 2

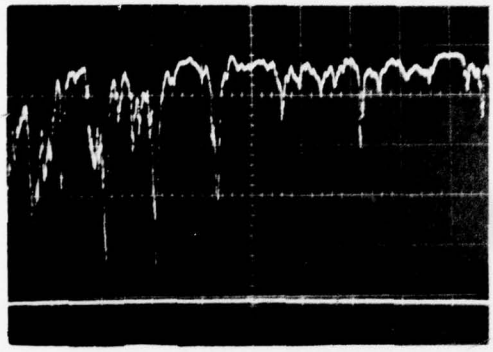

Channel 3

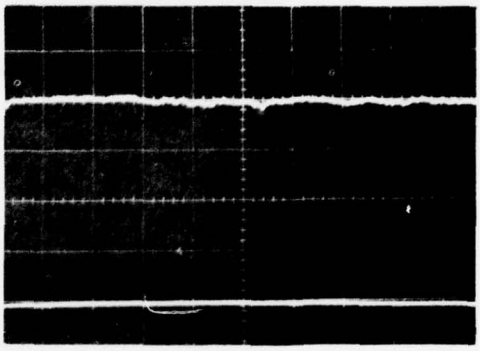

Channel 4

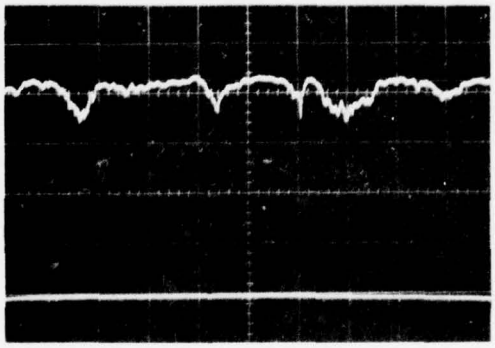

Channel 5

Figure 3-3. Oscillograms of pressure fluctuation recorded in Run E1 (Horizontal: 5 sec/div, Vertical: 0.5 V/div, Baseline: 1st from the bottom)

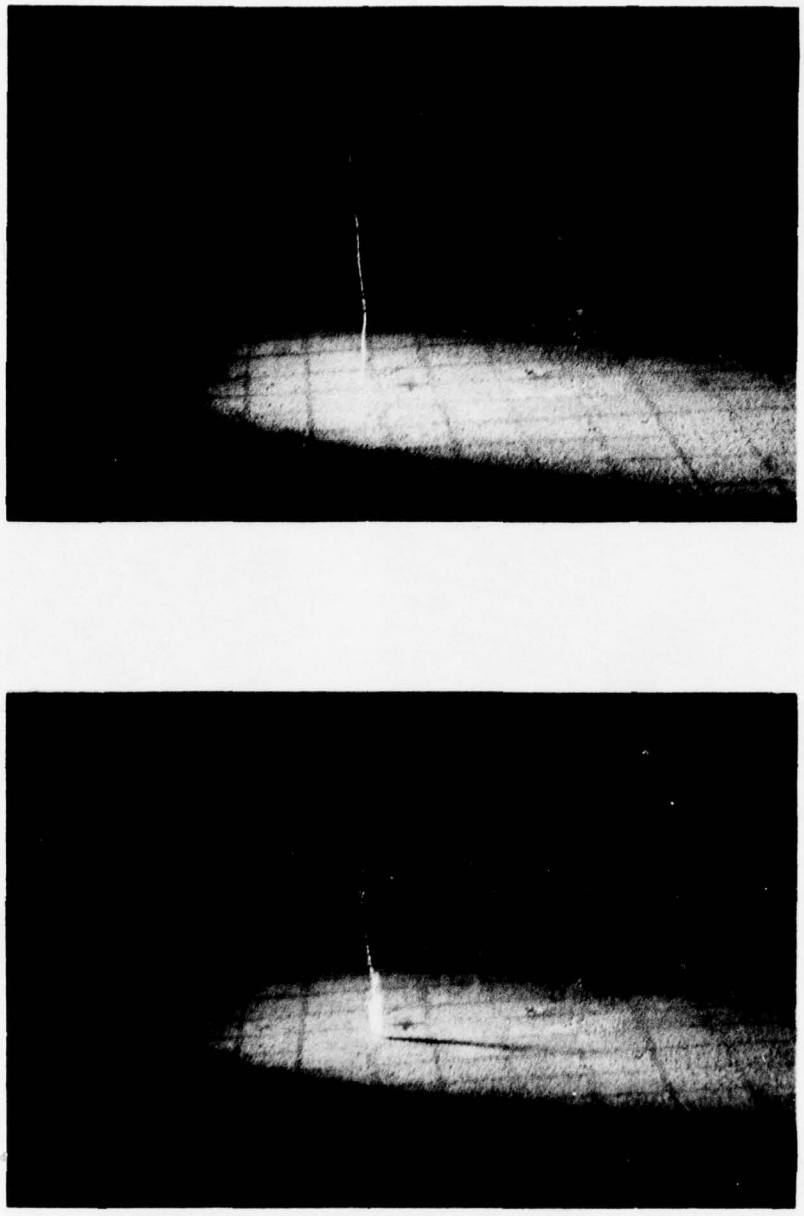

Figure 3-4. Typical floor vortices seen under the suction bell (Q_p = 660 cfs, El. = 110 ft, rectangular sump)

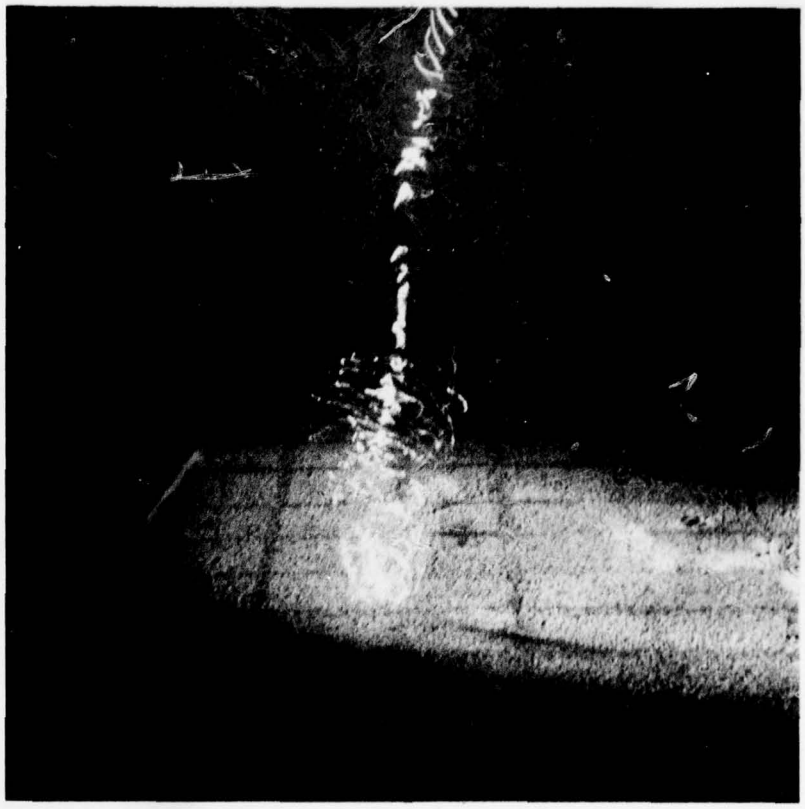

Figure 3-5. Close-up photographs of the floor vortices

(a) Run E2

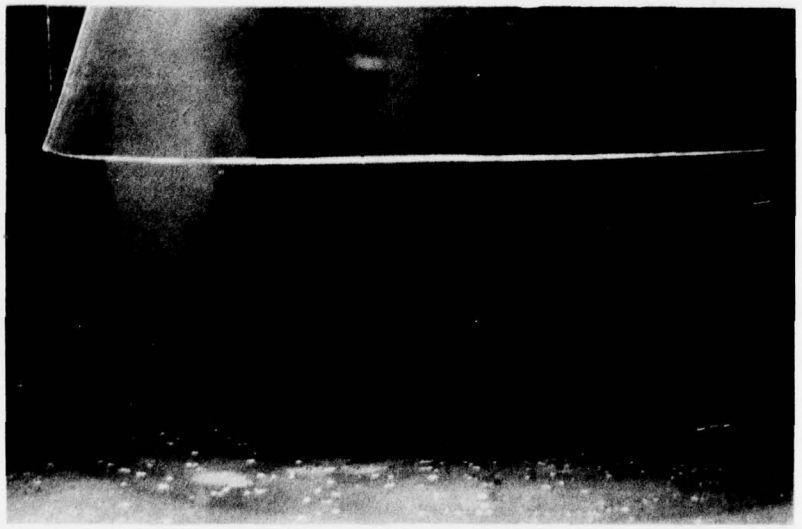

(b) Run E7

Figure 3-6. Typical floor vortices observed in Runs E2 and E7.

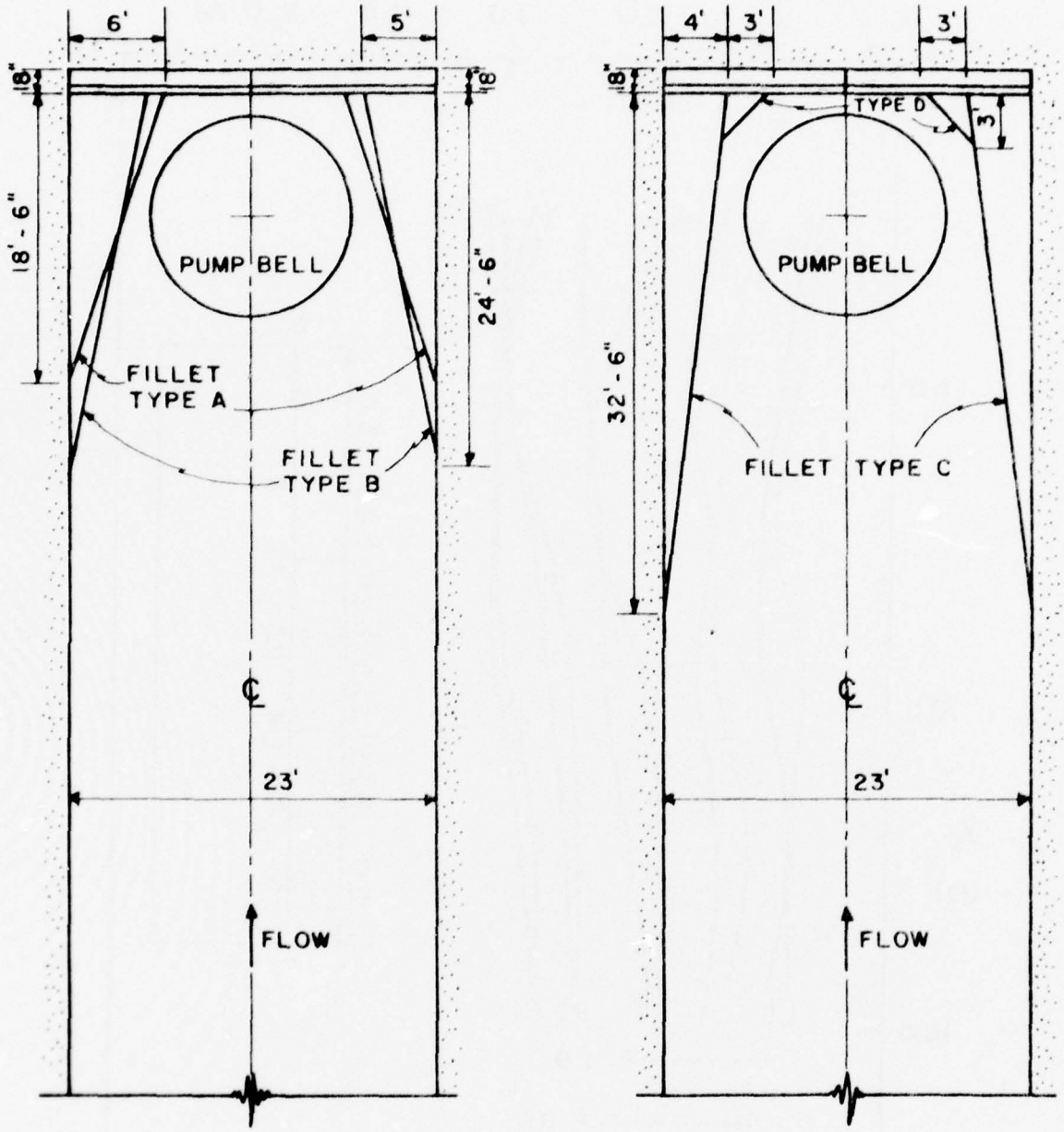

Figure 3-7. Geometrical configurations of various fillets

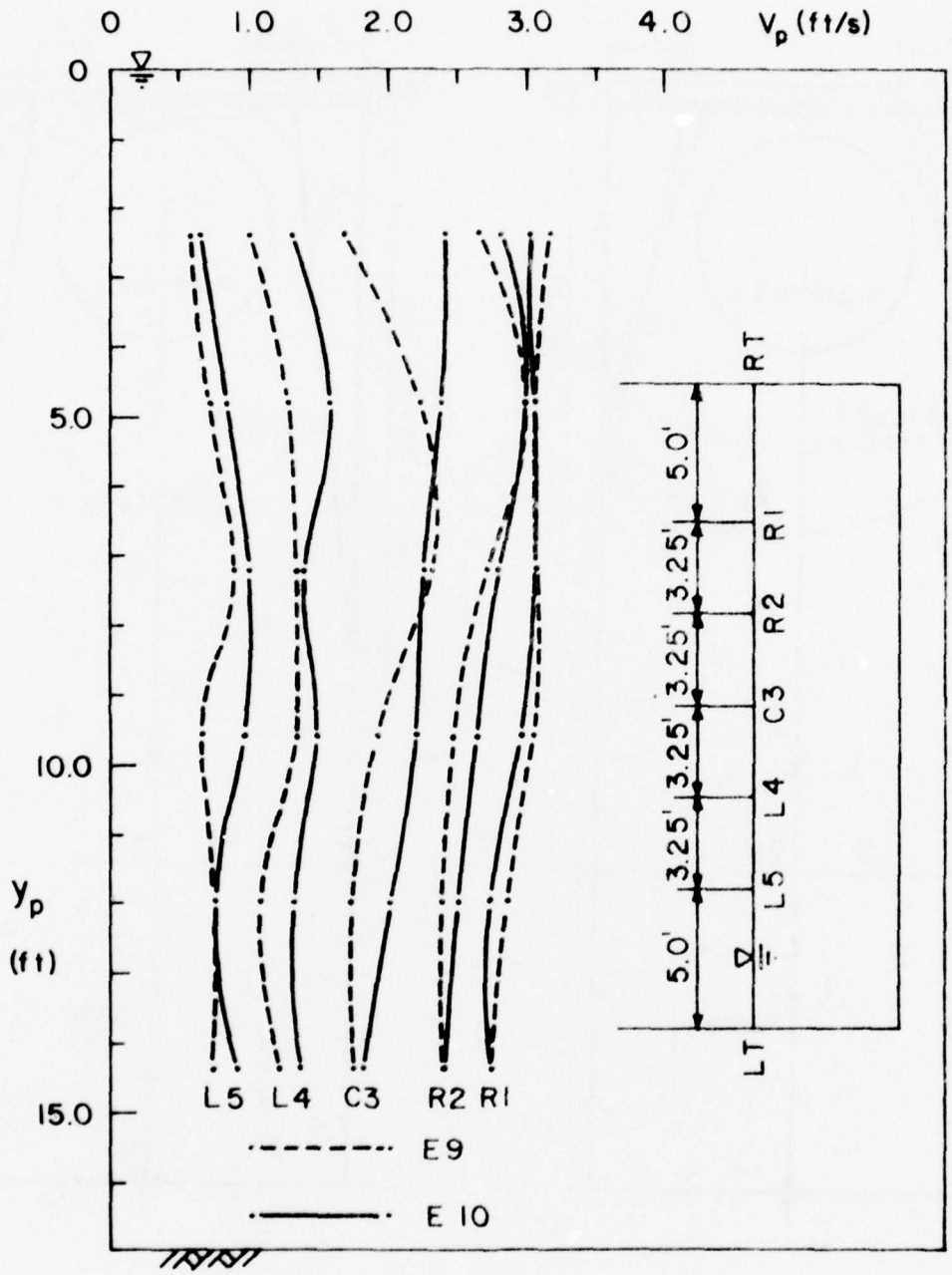

Figure 3-8. Velocity profiles obtained in Runs E9 and E10

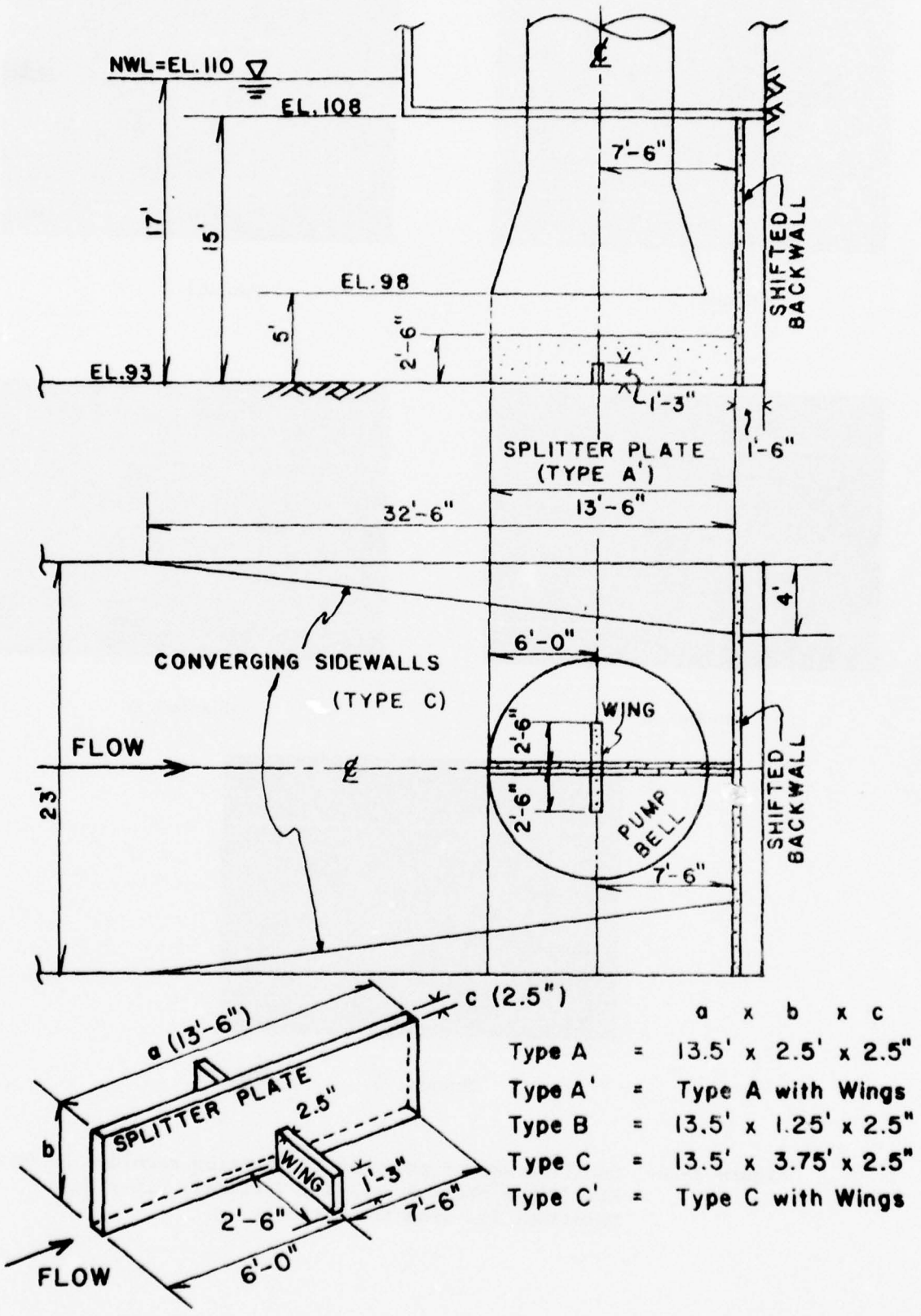

Figure 3-9. Dimensions of various splitter plates

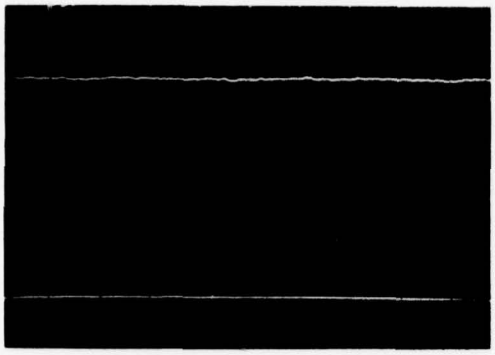

Channel 1

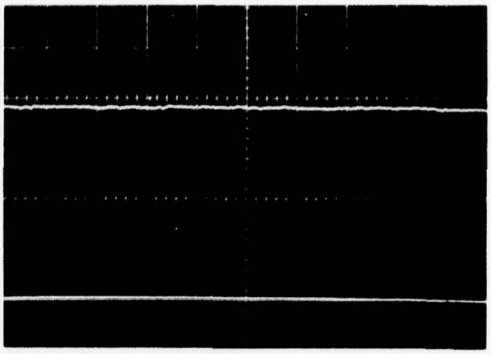

Channel 2

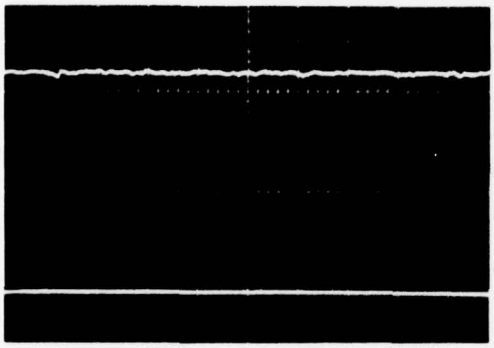

Channel 3

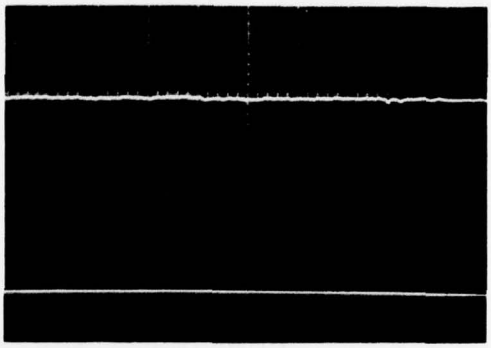

Channel 4

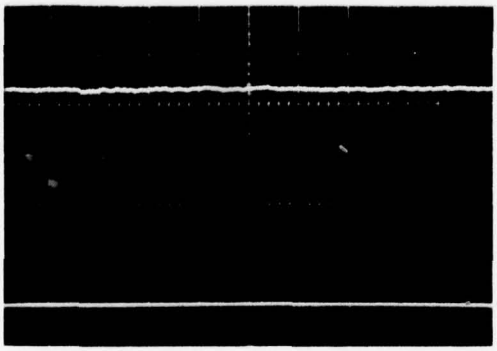

Channel 5

Figure 3-10. Oscillograms of pressure fluctuation recorded in Run E11 (Horizontal: 5 sec/div, Vertical: 0.5 V/div, Baseline: 1st from the bottom)

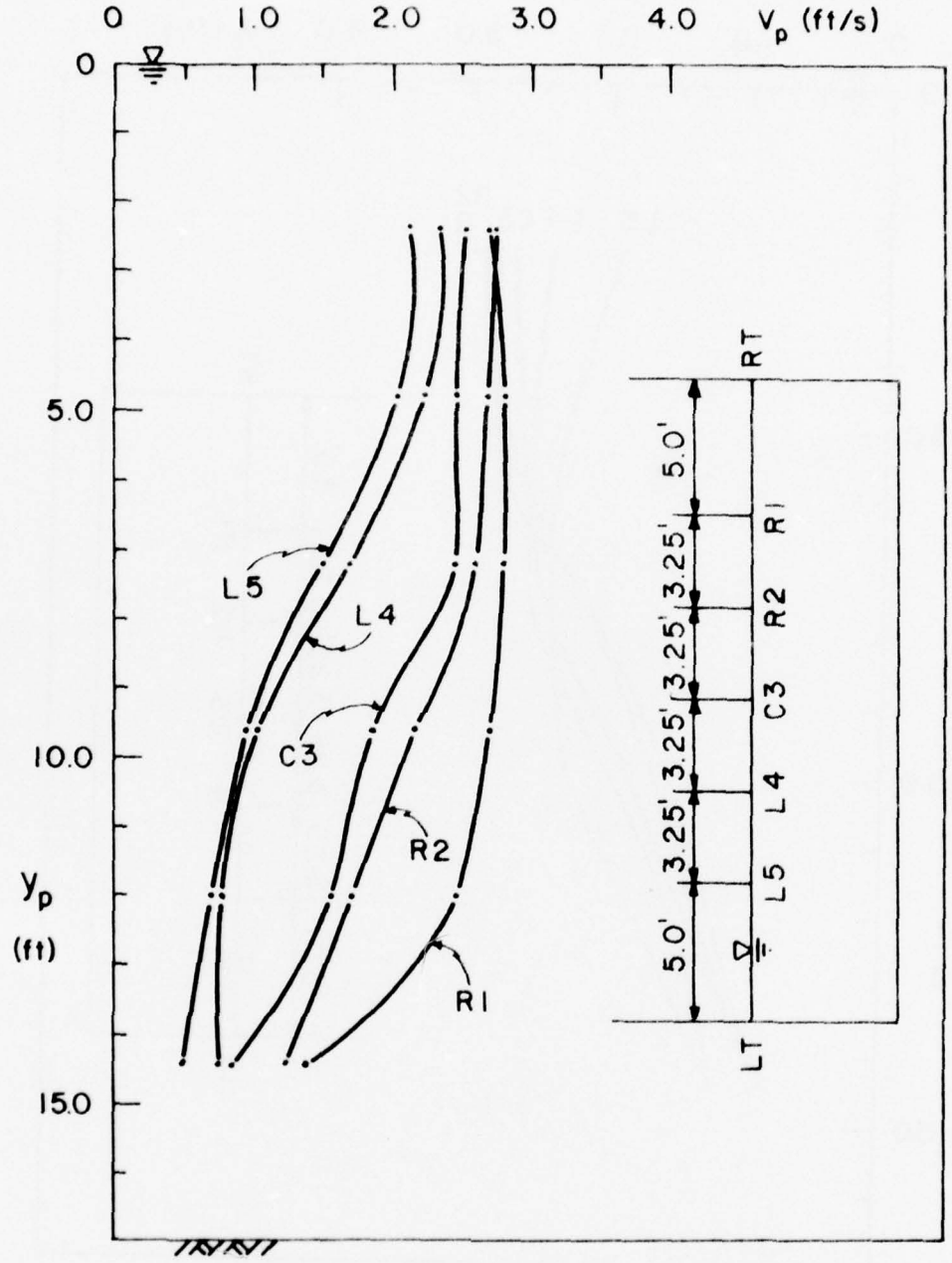

Figure 3-11. Velocity profiles obtained in Run E15' (with 12-in. deep trash rack, El. = 110 ft, Q_D = 660 cfs, backwall shift = 18 in., fillets = type C, splitter plate = type C')

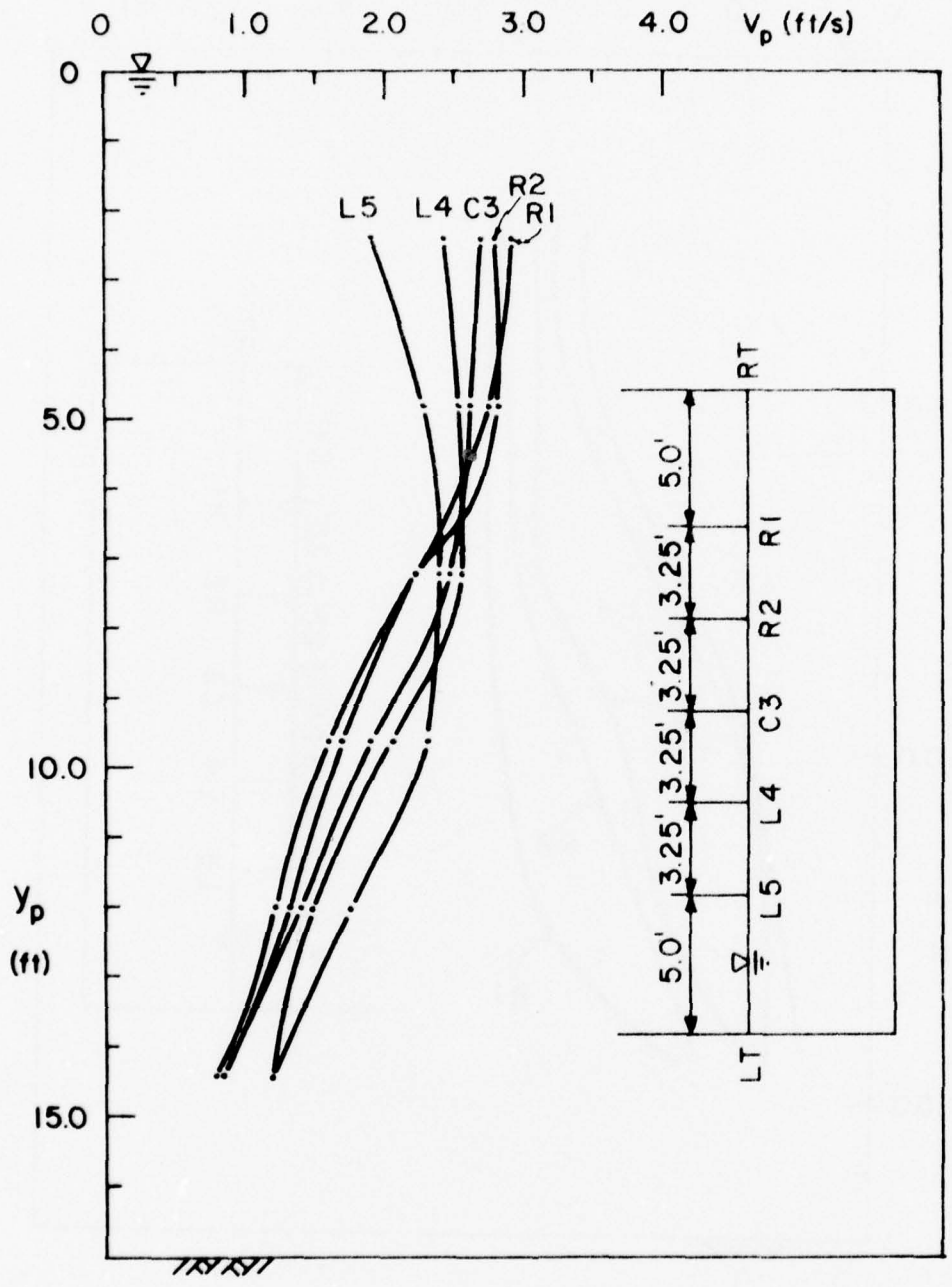

Figure 3-12. Velocity profiles obtained in Runs E15" (with 9-in. deep trash rack, El. = 110 ft, Q_p = 660 cfs, backwall shift = 18 in., fillets = type C, splitter plate = type A')

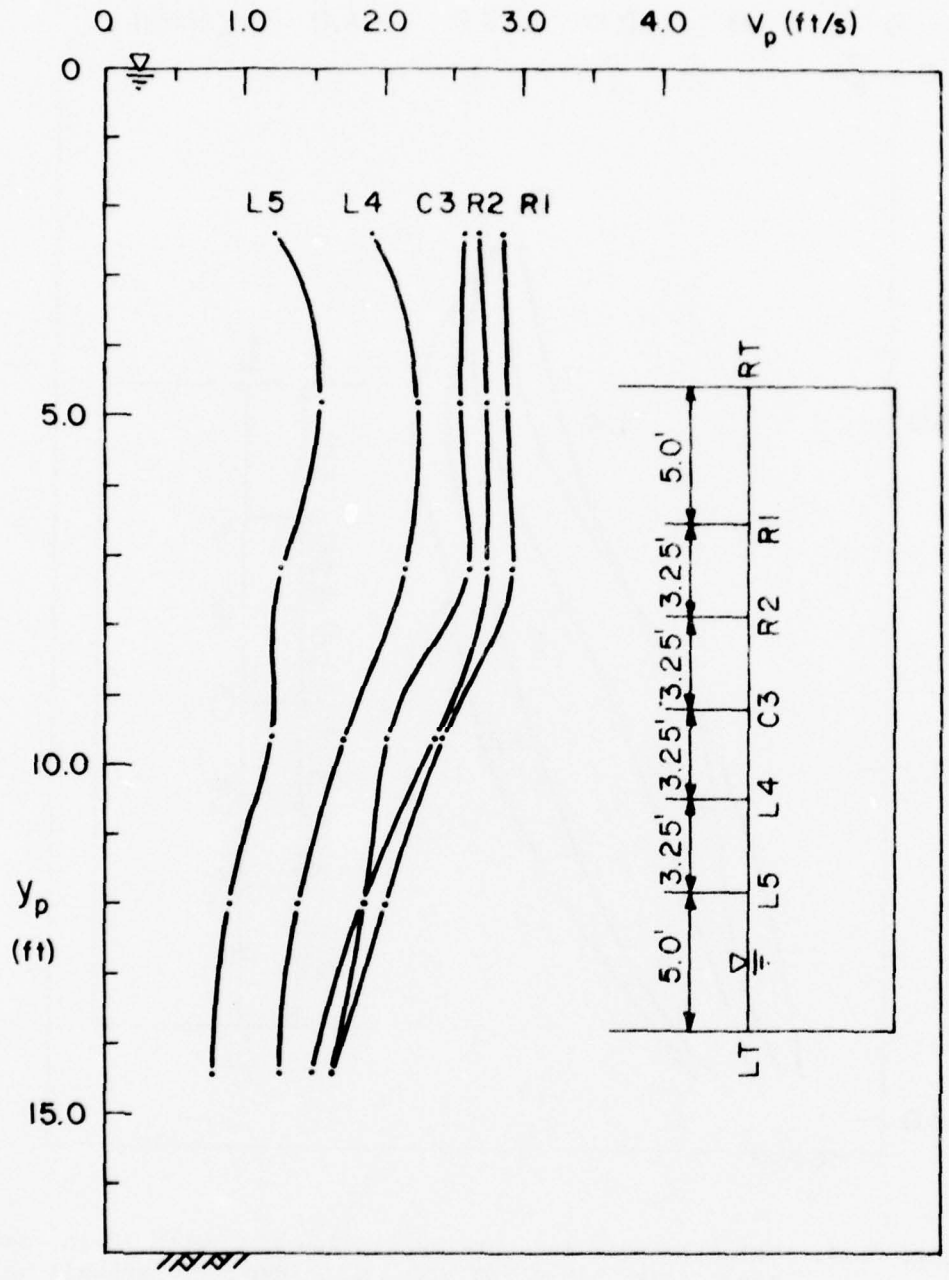

Figure 3-13. Velocity profiles obtained in Run 15''' (with 6-in. deep trash rack, El. = 110 ft, Q_p = 660 cfs, backwall shift = 18 in., fillets = type C, splitter plate = type C')

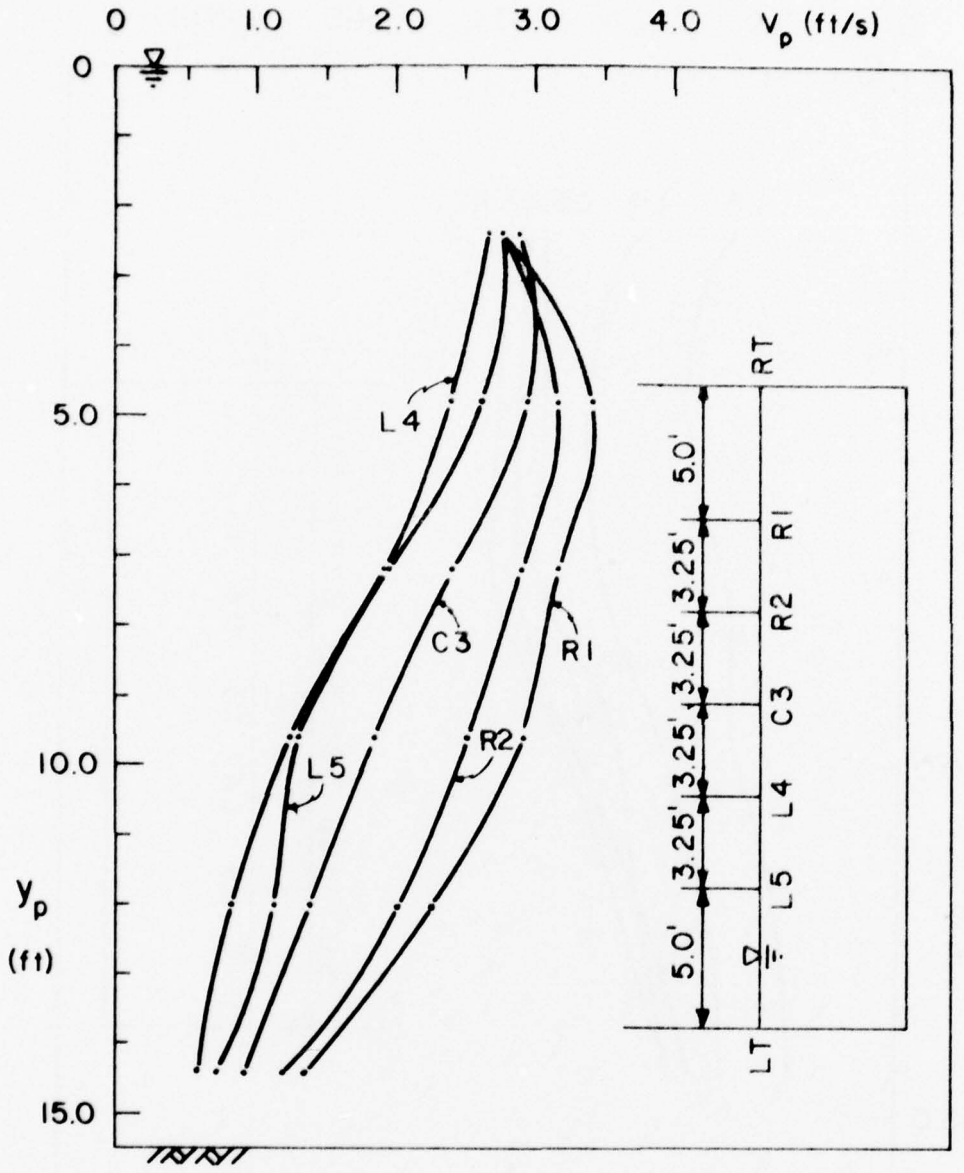

Figure 3-14. Velocity profiles obtained in Run E16 (with 12-in. deep trash rack, El. = 108.5 ft, Q_p = 660 cfs, backwall shift = 18 in., fillets = type C, splitter plate = type A')

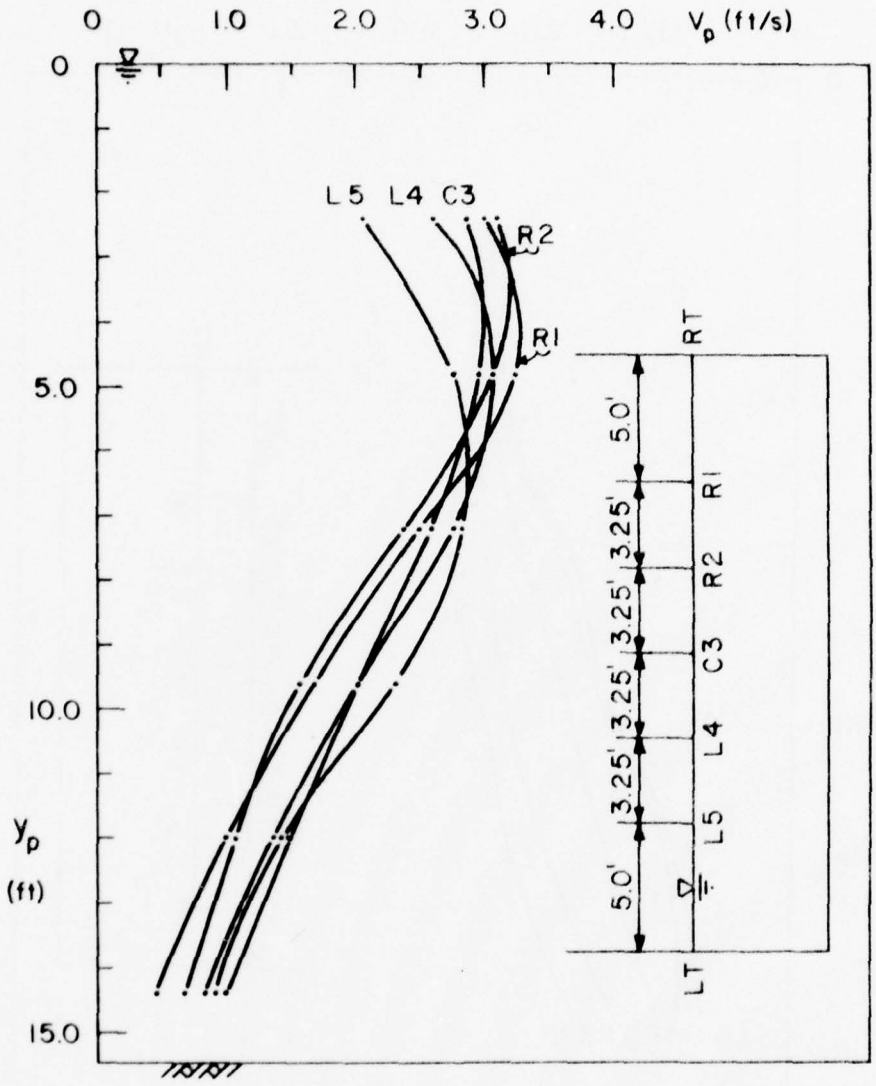

Figure 3-15. Velocity profiles obtained in Run E16' (with 9-in. deep trash rack, El. = 108.5 ft, Q_p = 660 cfs, backwall shift = 18 in., fillets = type C, splitter plate = type A')

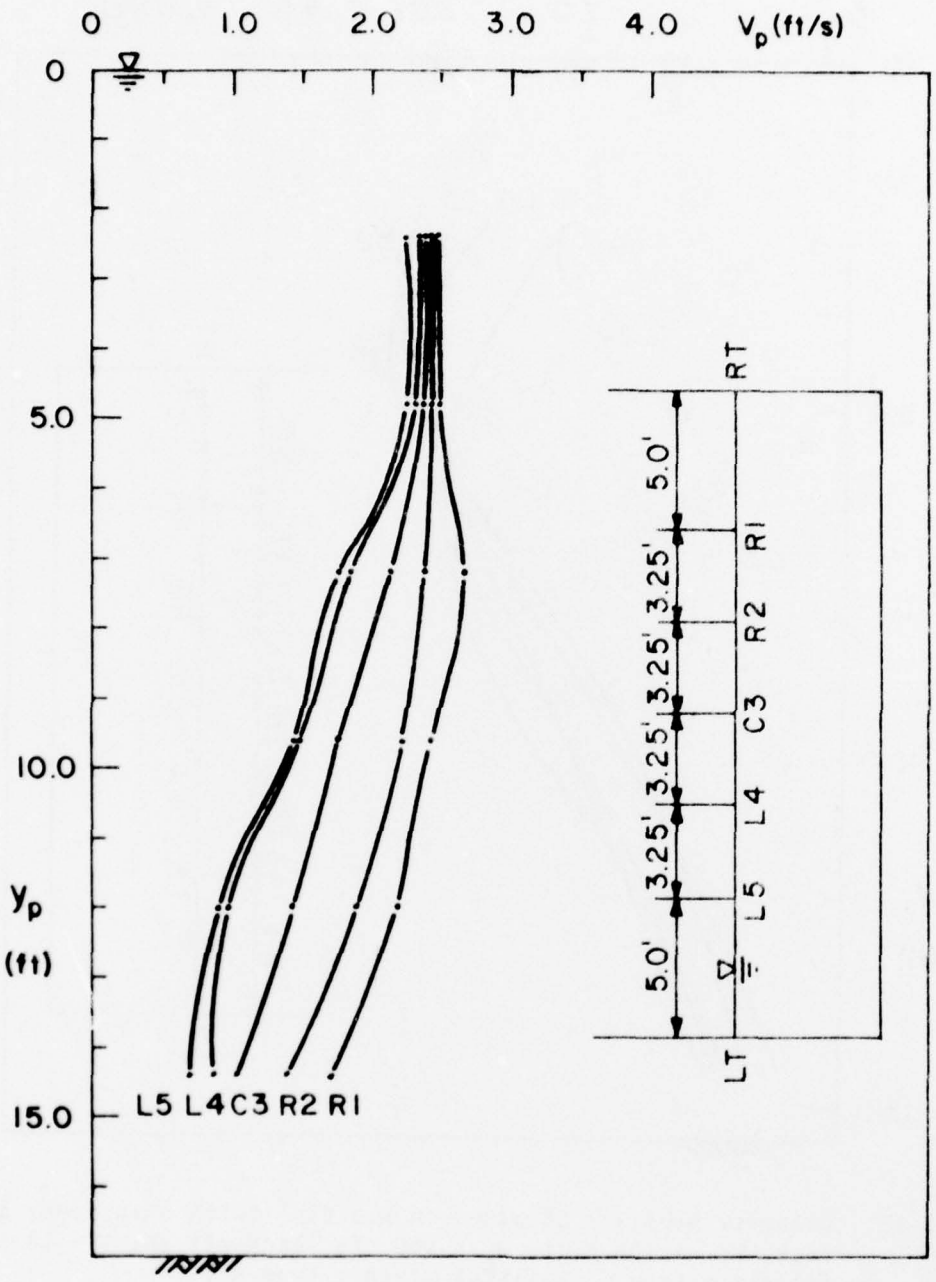

Figure 3-16. Velocity profiles obtained in Run E17 (with 12-in. deep trash rack, El. = 110 ft, Q_p = 600 cfs, backwall shift = 18 in., fillets = type C, splitter plate = type A')

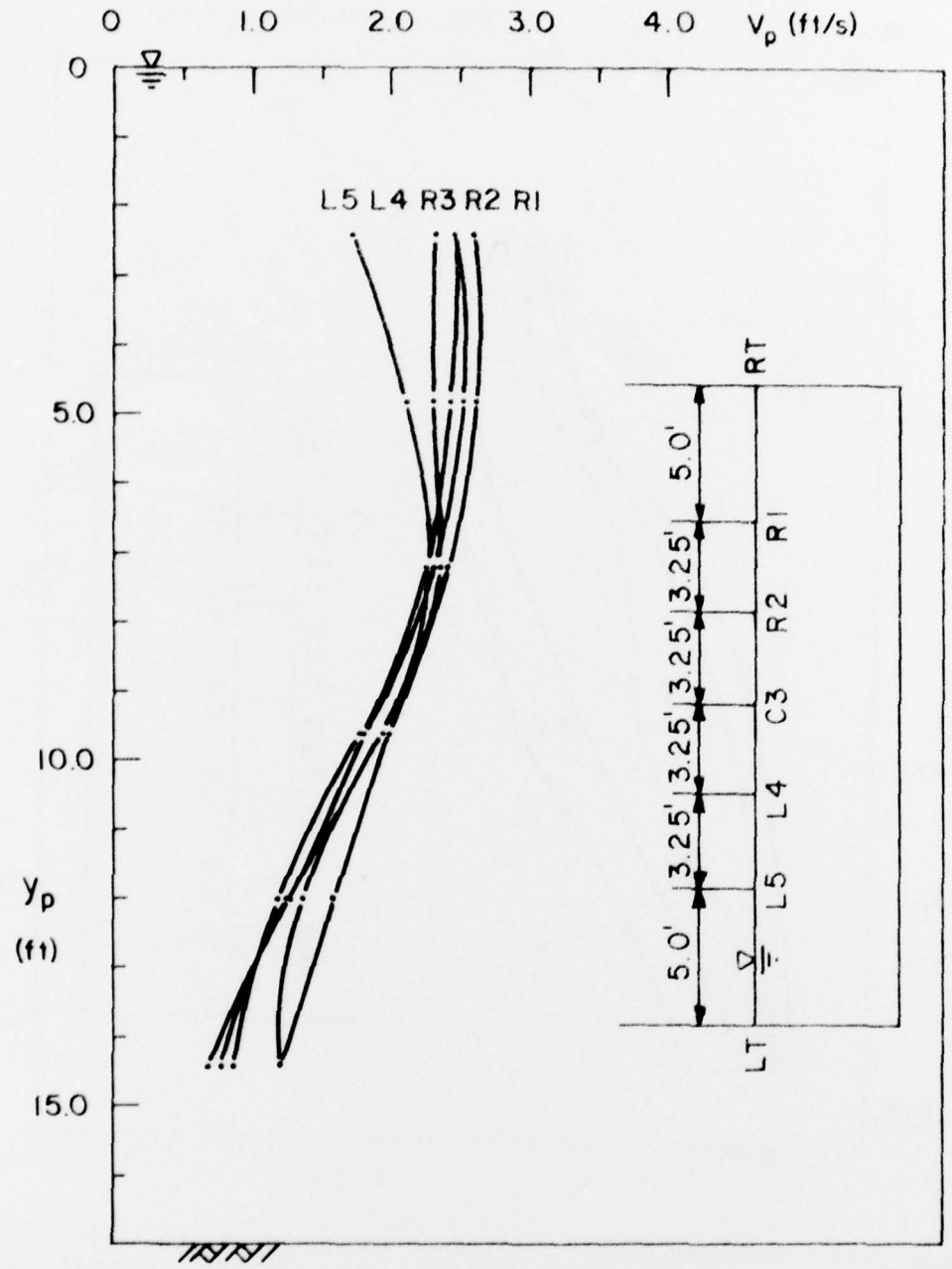

Figure 3-17. Velocity profiles obtained in Run E17' (with 9-in. deep trash rack, El. = 110 ft, Q_p = 600 cfs, backwall shift = 18 in., fillets = type C, splitter plate = type A')

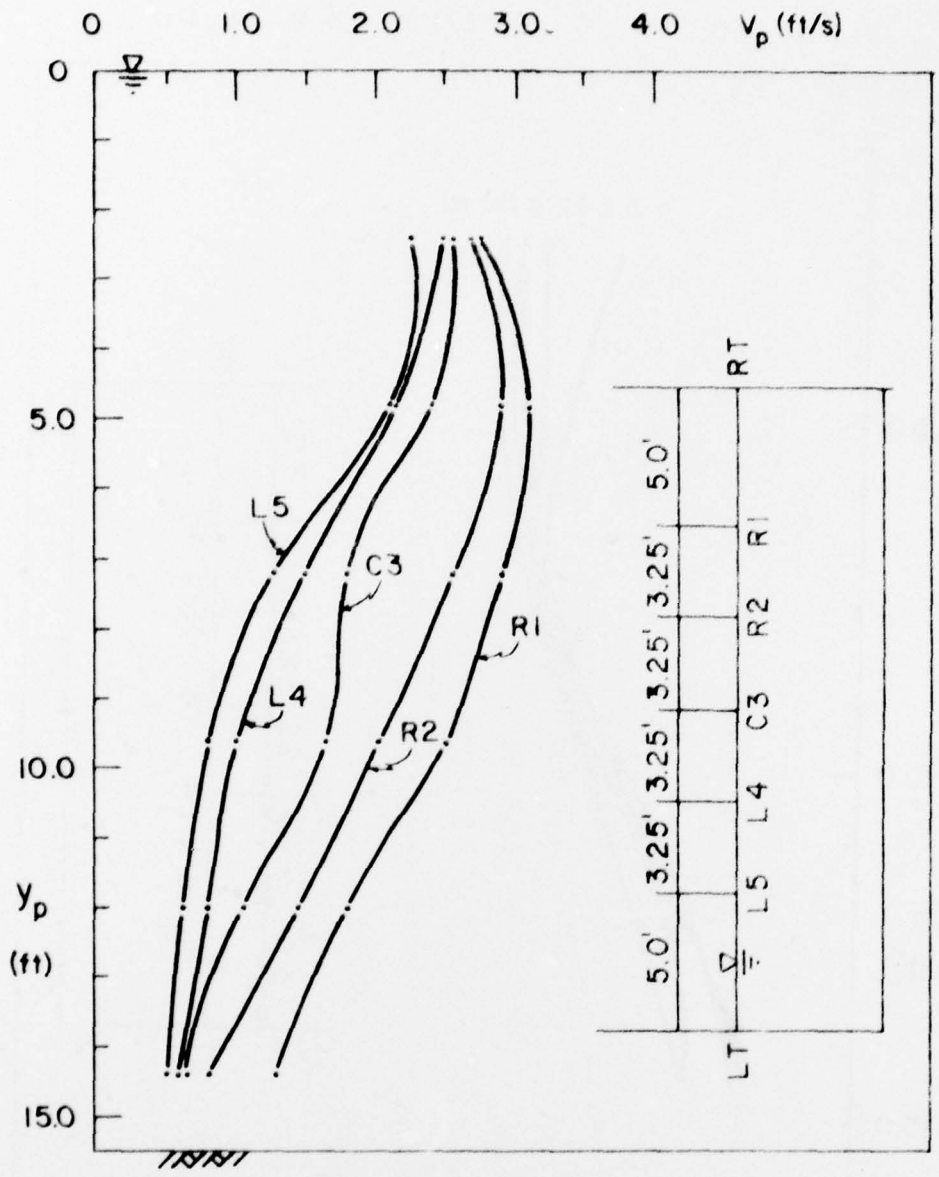

Figure 3-18. Velocity profiles obtained in Run E18 (with 12-in. deep trash rack, El. = 108.5 ft, Q_p = 600 cfs, backwall shift = 18 in., fillets = type C, splitter plate = type A')

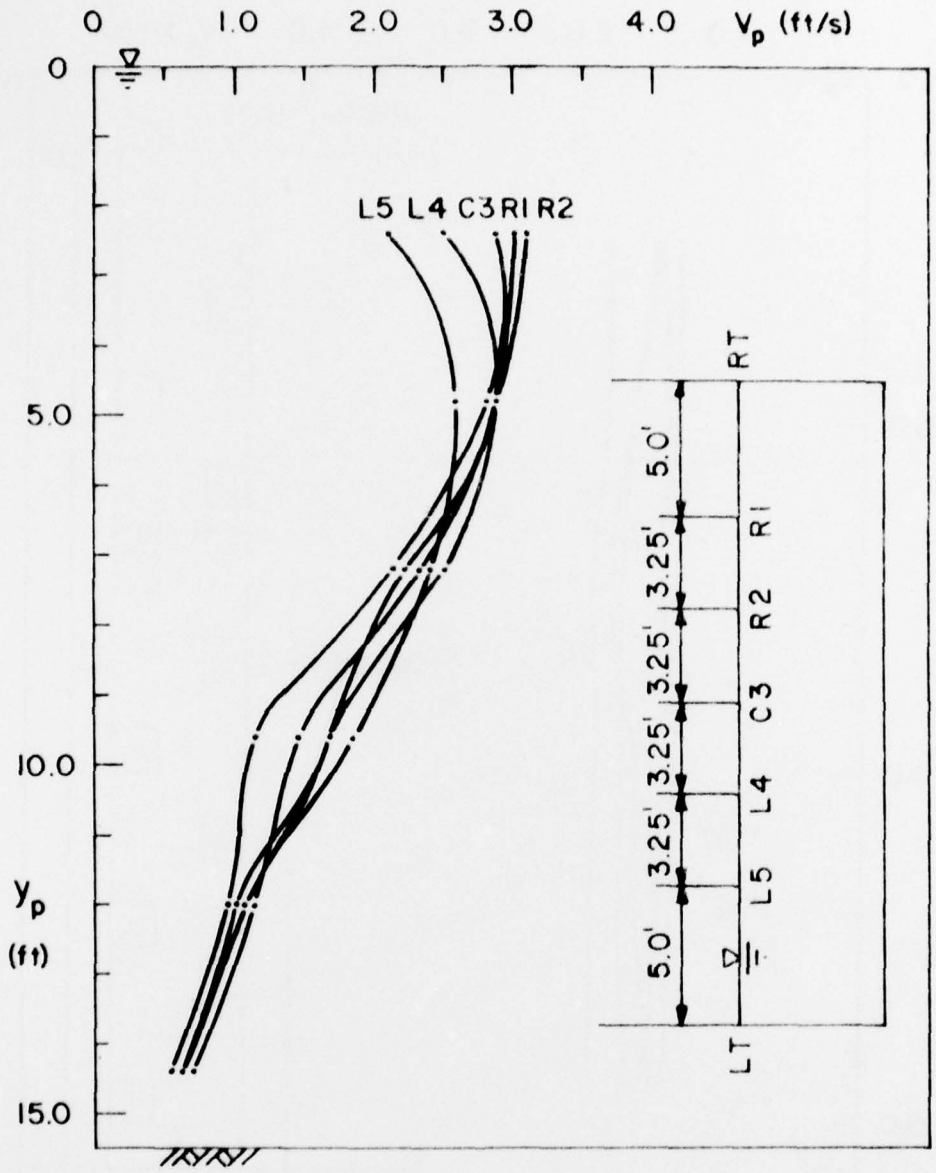

Figure 3-19. Velocity profiles obtained in Run E18' (with 9-in. deep trash rack, El. = 108.5 ft, Q_p = 600 cfs, backwall shift = 18 in., fillets = type C, splitter plate = type A')

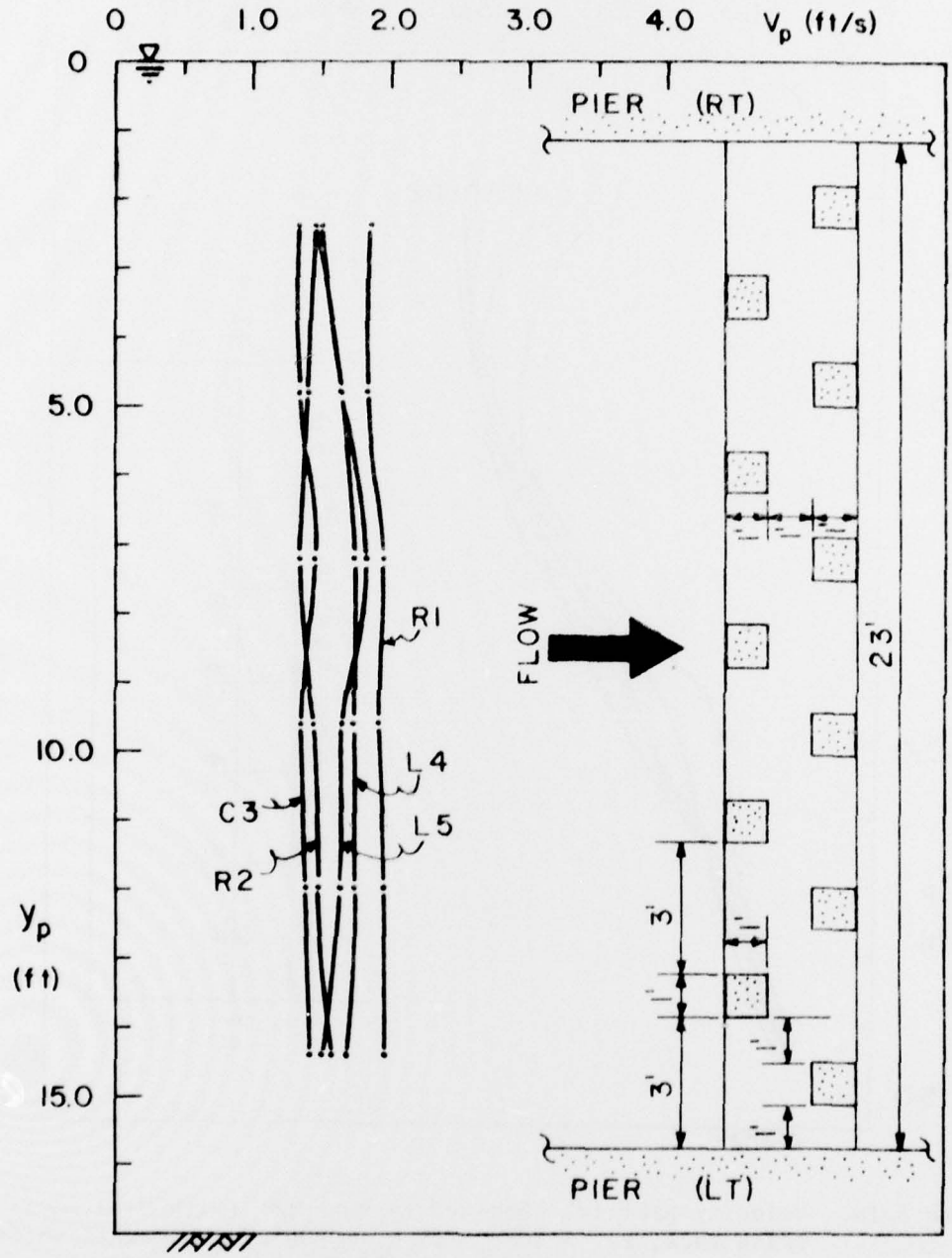

Figure 3-20. Velocity profiles obtained in Run E20 with baffle blocks installed in the sump (with 1.5-in. deep trash rack, El. = 110 ft, Q_p = 600 cfs, rectangular sump)

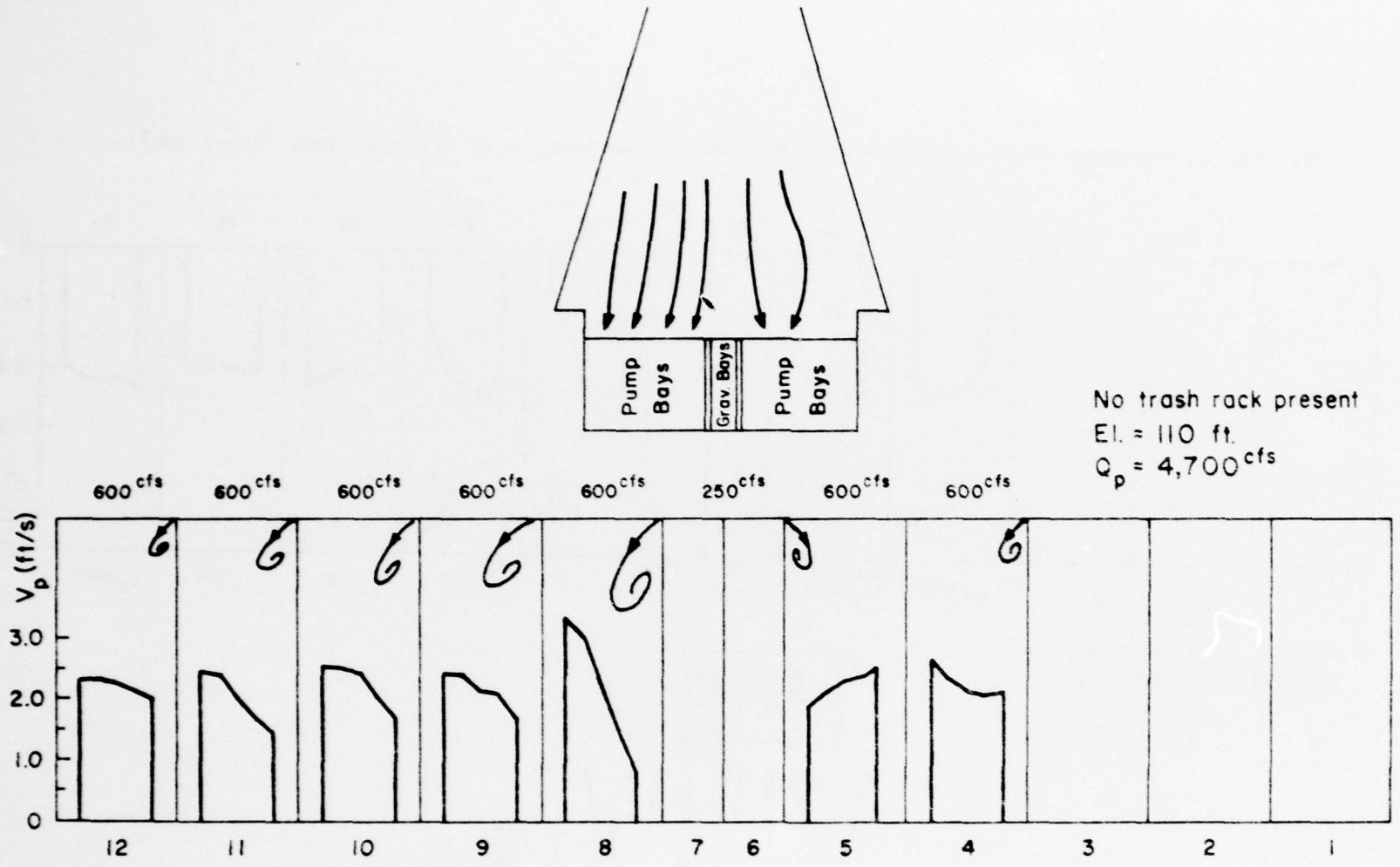

Figure 3-21. Mean velocity distributions in pump sumps (no gravity-bay piers extended)

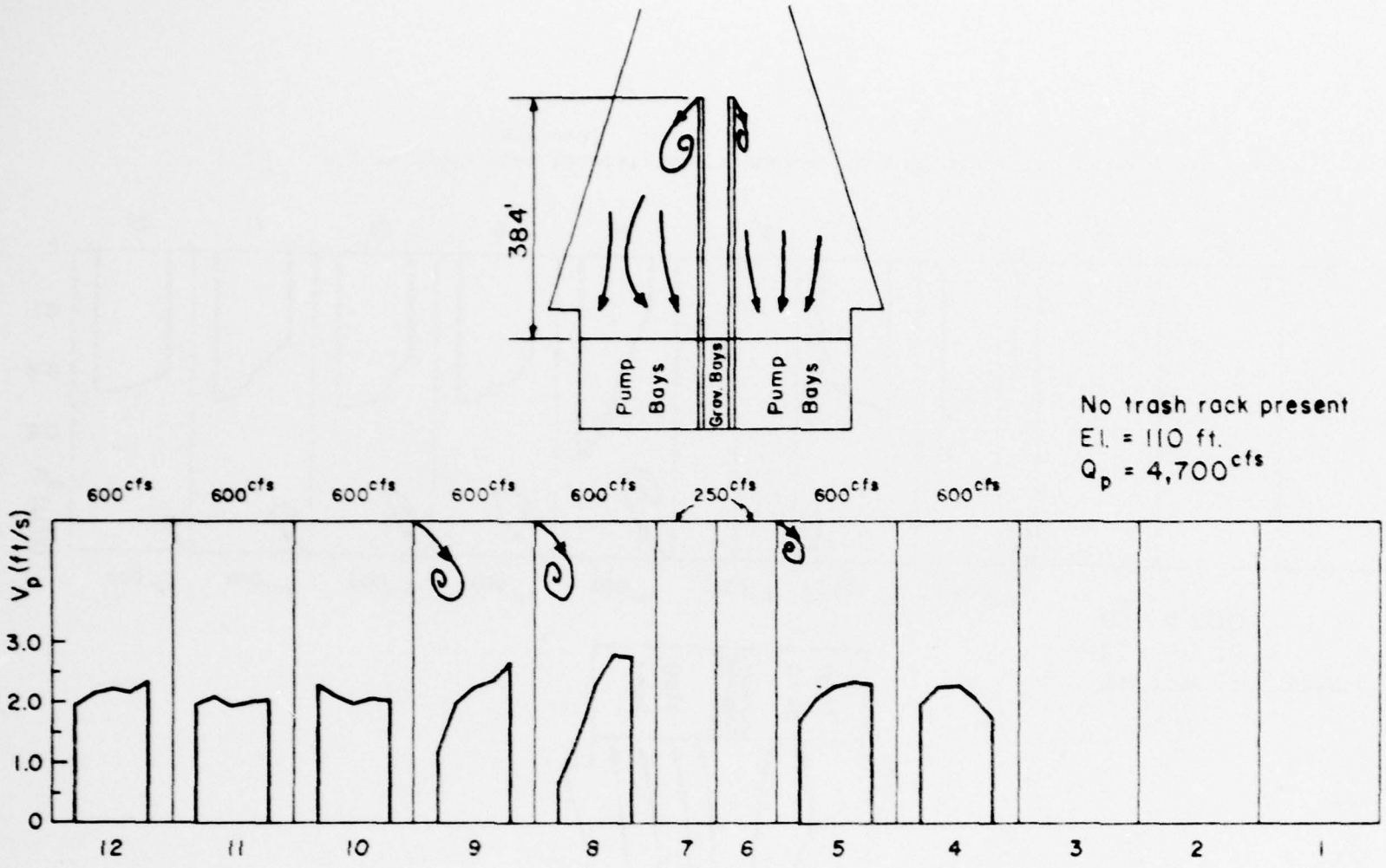

Figure 3-22. Mean velocity distributions in pump sumps (gravity-bay piers extended by 384 ft)

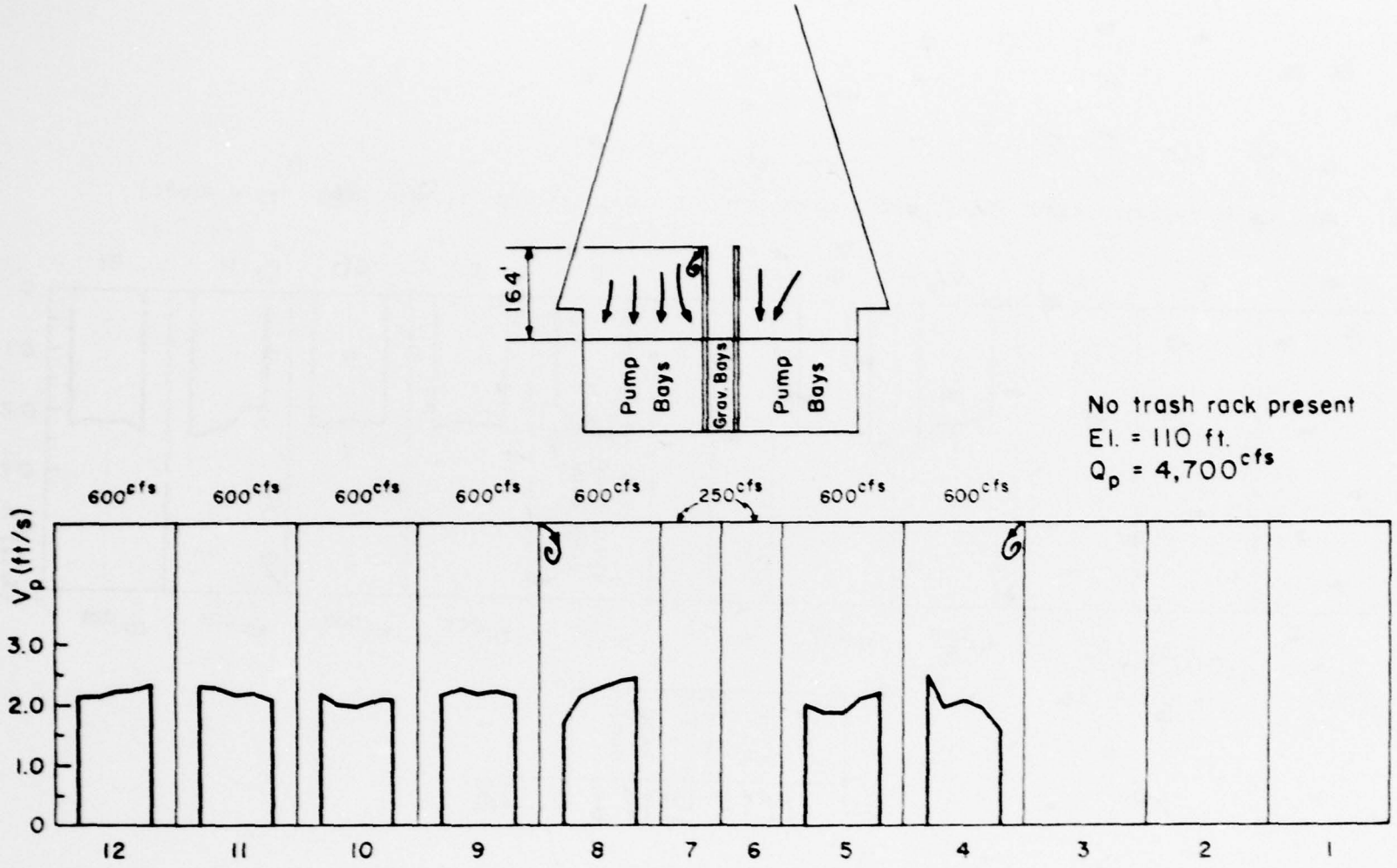

Figure 3-23. Mean velocity distributions in pump sumps (gravity-bay piers extended by 164 ft)

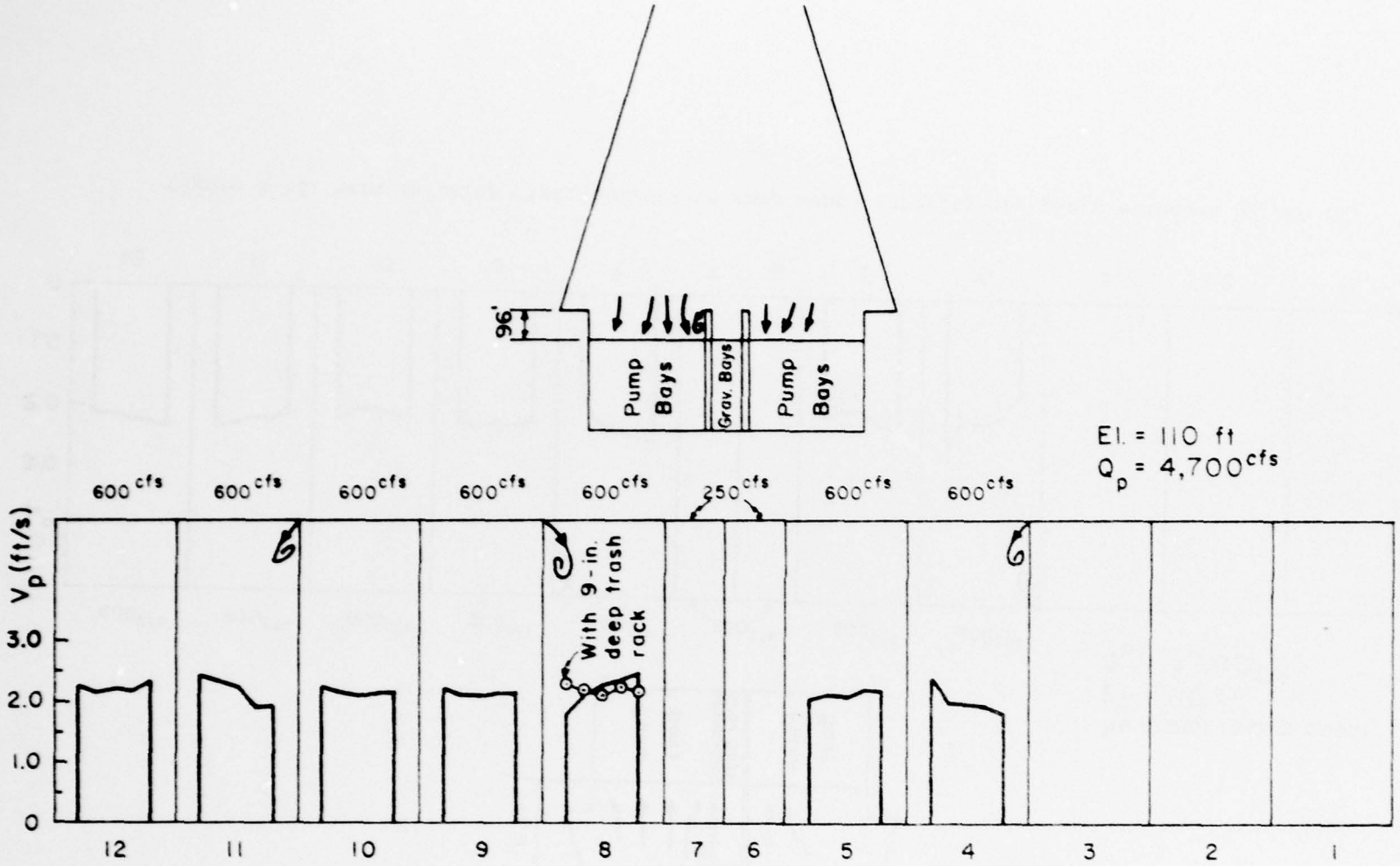

Figure 3-24. Mean velocity distributions in pump sumps (gravity-bay piers extended by 96 ft)

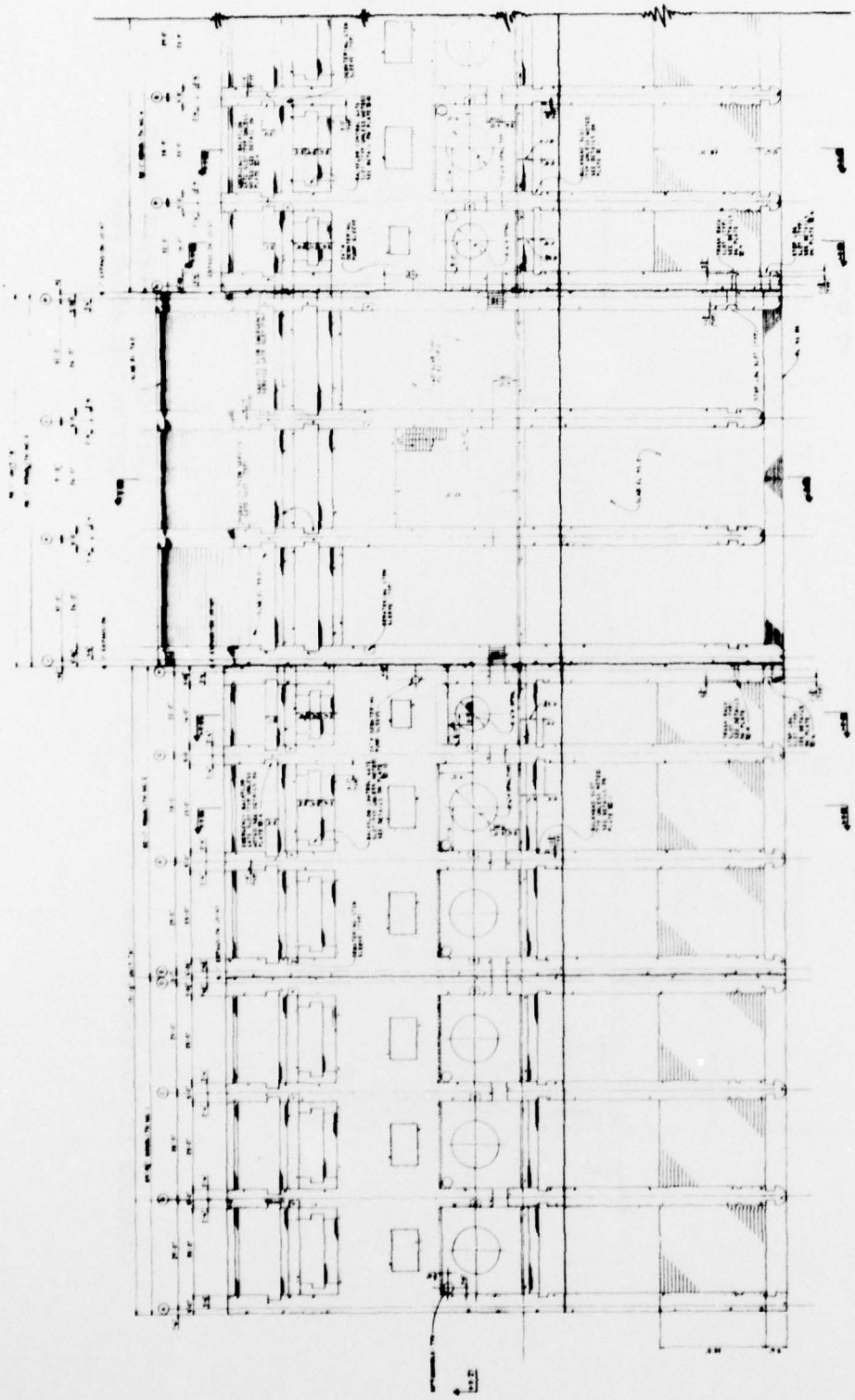

APPENDIX I Plan at Elevation 118.0

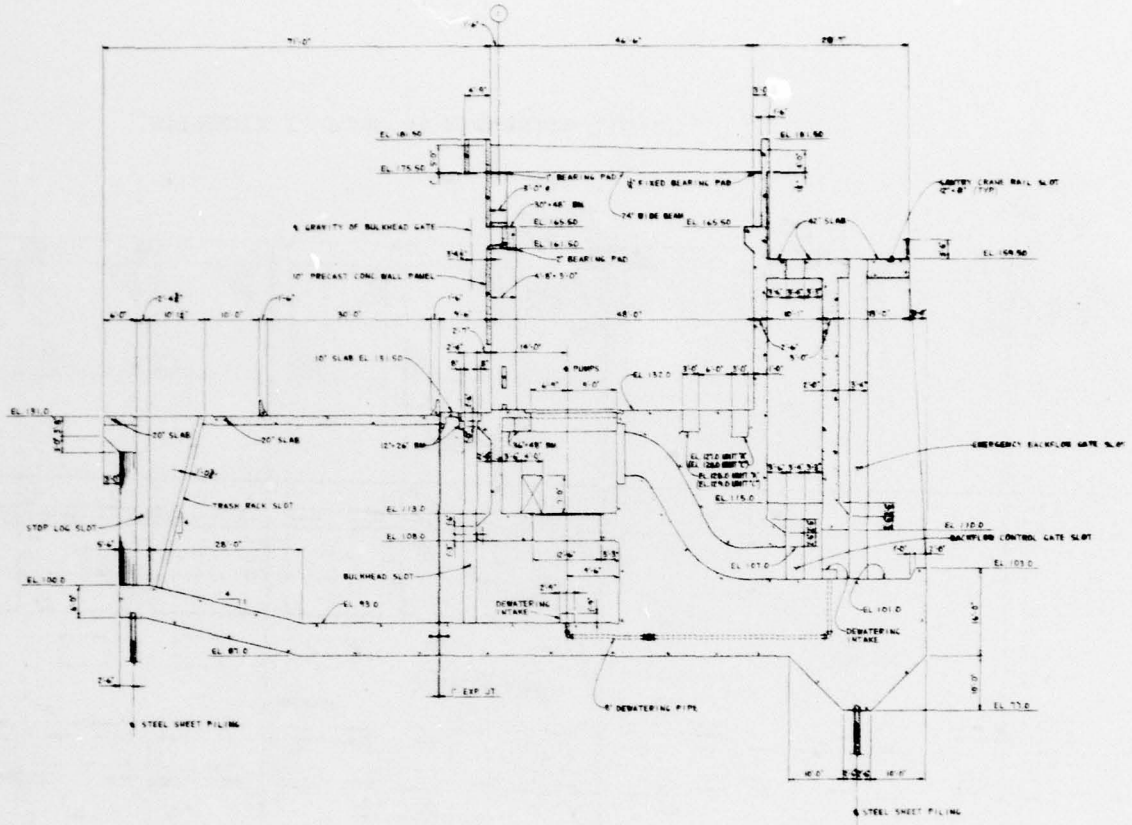

APPENDIX II Section through 600 cfs Pump bay

LAKE CHICOT PUMPING PLANT
SECTION THRU 600 cfs PUMP BAY

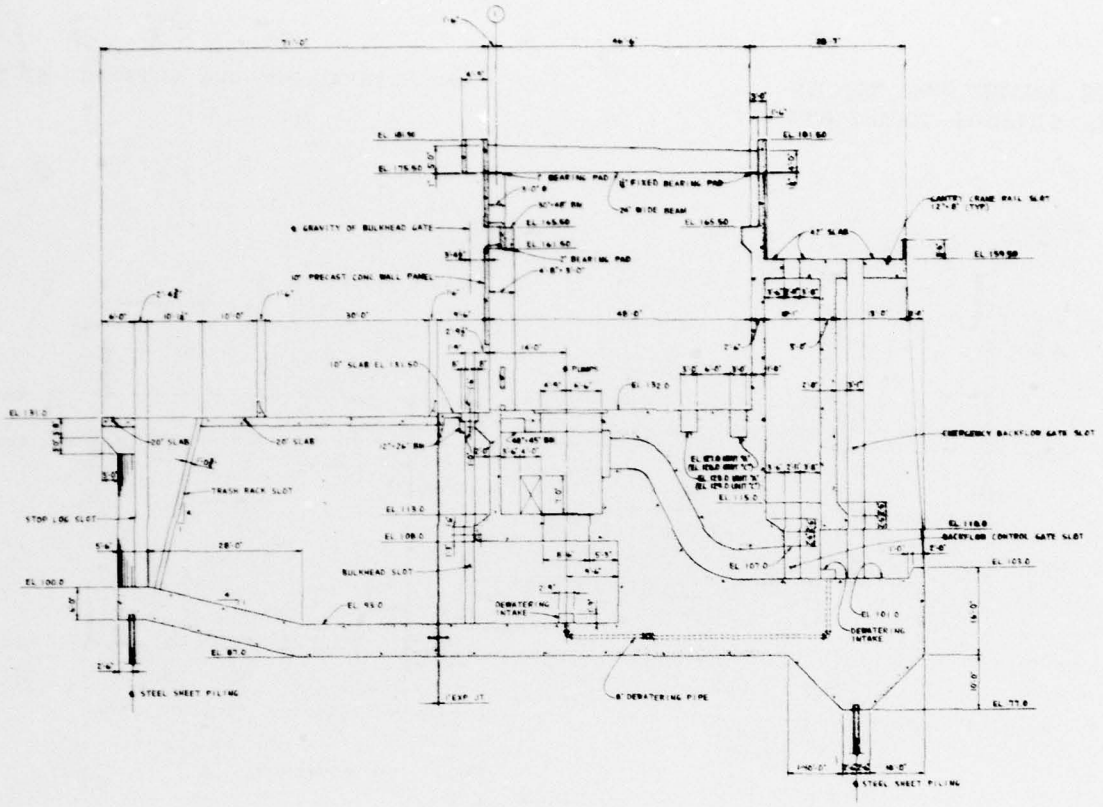

APPENDIX III Section through 250 cfs pump bay

LAKE CHICOT PUMPING PLANT
SECTION THRU 250 cfs PUMP BAY

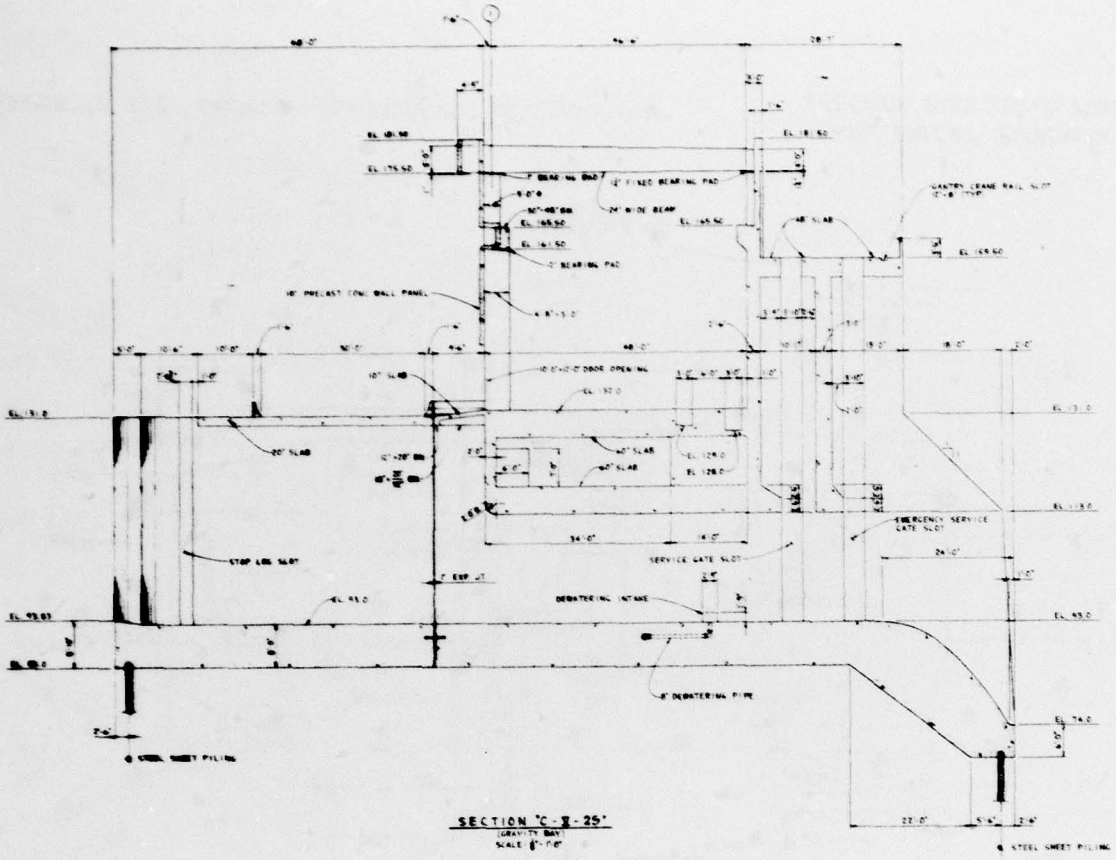

APPENDIX IV Section through gravity bay

LAKE CHICOT PUMPING PLANT
SECTION THRU GRAVITY BAY

BIBLIOGRAPHIC DATA SHEET	1. Report No. IIHR Rept 208	2.	3. Recipient's Accession No.
4. Title and Subtitle Detailed Model Study of Pump Approach Flows for the Lake Chicot Pumping Plant			5. Report Date Oct 1977 6.
7. Author(s) Tatsuaki Nakato and J.F. Kennedy			8. Performing Organization Rept. No.
9. Performing Organization Name and Address Institute of Hydraulic Research The University of Iowa Iowa City, IA 52242			10. Project/Task/Work Unit No. 11. Contract/Grant No.
12. Sponsoring Organization Name and Address Stanley Consultants, Inc Muscatine, IA			13. Type of Report & Period Covered 14.

15. Supplementary Notes

16. Abstracts A 1:24 Froude-scale model of the proposed Lake Chicot Pumping Station was constructed and utilized to identify and to correct hydraulically objectionable features of the flows in the pump sumps. The model tests showed that the flows from the plant forebay generally enter the individual pump bays with a strong transverse component of velocity and produced on an intense captive eddy on the lee side of each pump-bay partition wall. The transverse velocity resulted from geometric constraints imposed on the plant configuration. In order to achieve better pump approach-flow conditions trash racks with relatively deep vertical bars which functioned as turning vanes were proposed. A 1:10-scale sump model then was built to test for model-scale effects in the trash-rack tests, and an extensive study was conducted to obtain an improved sump configuration which would minimize any vortex-related problems in and around pump suction bells. The modified sump configuration has small clearance between the pump bell and sump back-wall; converging sidewalls; and a floor mounted splitter plate (vortex breaker) beneath the pump.

17. Key Words and Document Analysis. 17a. Descriptors
model study, pump approach flows, pumping plant

17b. Identifiers/Open-Ended Terms

17c. COSATI Field/Group

18. Availability Statement	DISTRIBUTION STATEMENT A Approved for public release; Distribution Unlimited	19. Security Class (This Report) UNCLASSIFIED	21. No. of Pages 63
		20. Security Class (This Page) UNCLASSIFIED	22. Price

INSTRUCTIONS FOR COMPLETING FORM NTIS-35 (Bibliographic Data Sheet based on COSATI Guidelines to Format Standards for Scientific and Technical Reports Prepared by or for the Federal Government, PB-180 600).

1. **Report Number.** Each individually bound report shall carry a unique alphanumeric designation selected by the performing organization or provided by the sponsoring organization. Use uppercase letters and Arabic numerals only. Examples FASEB-NS-73-87 and FAA-RD-73-09.

2. Leave blank.

3. **Recipient's Accession Number.** Reserved for use by each report recipient.

4. **Title and Subtitle.** Title should indicate clearly and briefly the subject coverage of the report, subordinate subtitle to the main title. When a report is prepared in more than one volume, repeat the primary title, add volume number and include subtitle for the specific volume.

5. **Report Date.** Each report shall carry a date indicating at least month and year. Indicate the basis on which it was selected (e.g., date of issue, date of approval, date of preparation, date published).

6. **Performing Organization Code.** Leave blank.

7. **Author(s).** Give name(s) in conventional order (e.g., John R. Doe, or J.Robert Doe). List author's affiliation if it differs from the performing organization.

8. **Performing Organization Report Number.** Insert if performing organization wishes to assign this number.

9. **Performing Organization Name and Mailing Address.** Give name, street, city, state, and zip code. List no more than two levels of an organizational hierarchy. Display the name of the organization exactly as it should appear in Government indexes such as Government Reports Index (GRI).

10. **Project/Task/Work Unit Number.** Use the project, task and work unit numbers under which the report was prepared.

11. **Contract/Grant Number.** Insert contract or grant number under which report was prepared.

12. **Sponsoring Agency Name and Mailing Address.** Include zip code. Cite main sponsors.

13. **Type of Report and Period Covered.** State interim, final, etc., and, if applicable, inclusive dates.

14. **Sponsoring Agency Code.** Leave blank.

15. **Supplementary Notes.** Enter information not included elsewhere but useful, such as: Prepared in cooperation with . . . Translation of . . . Presented at conference of . . . To be published in . . . Supersedes . . . Supplements . . . Cite availability of related parts, volumes, phases, etc. with report number.

16. **Abstract.** Include a brief (200 words or less) factual summary of the most significant information contained in the report. If the report contains a significant bibliography or literature survey, mention it here.

17. **Key Words and Document Analysis. (a). Descriptors.** Select from the Thesaurus of Engineering and Scientific Terms the proper authorized terms that identify the major concept of the research and are sufficiently specific and precise to be used as index entries for cataloging.

(b). Identifiers and Open-Ended Terms. Use identifiers for project names, code names, equipment designators, etc. Use open-ended terms written in descriptor form for those subjects for which no descriptor exists.

(c). COSATI Field/Group. Field and Group assignments are to be taken from the 1964 COSATI Subject Category List. Since the majority of documents are multidisciplinary in nature, the primary Field/Group assignment(s) will be the specific discipline, area of human endeavor, or type of physical object. The application(s) will be cross-referenced with secondary Field/Group assignments that will follow the primary posting(s).

18. **Distribution Statement.** Denote public releasability, for example "Release unlimited", or limitation for reasons other than security. Cite any availability to the public, other than NTIS, with address, order number and price, if known.

19 & 20. **Security Classification.** Do not submit classified reports to the National Technical Information Service.

21. **Number of Pages.** Insert the total number of pages, including introductory pages, but excluding distribution list, if any.

22. **NTIS Price.** Leave blank.